Packing and flow particle simulations

Seminar to the Engineering Faculty

Pontificia Universidad Javeriana, Bogota, Colombia

July 29th, 2022

A P Santos

Analytical Mechanics Associates, Inc.

NASA Ames Research Center, Moffett Field, California USA

Rolling and Twisting friction matter for hopper flow

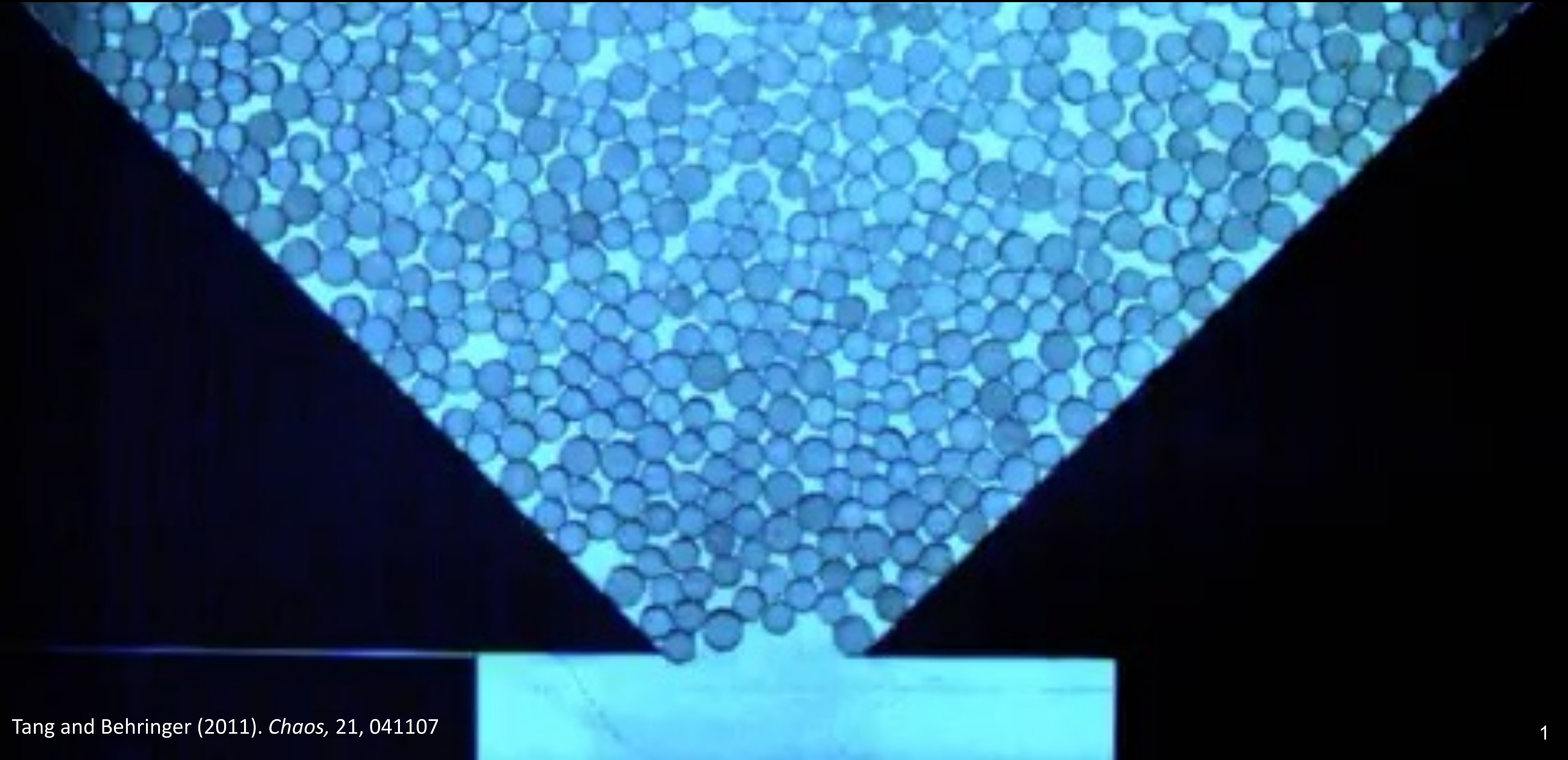

Tang and Behringer (2011). *Chaos,* 21, 041107

Rover performance depends on regolith properties

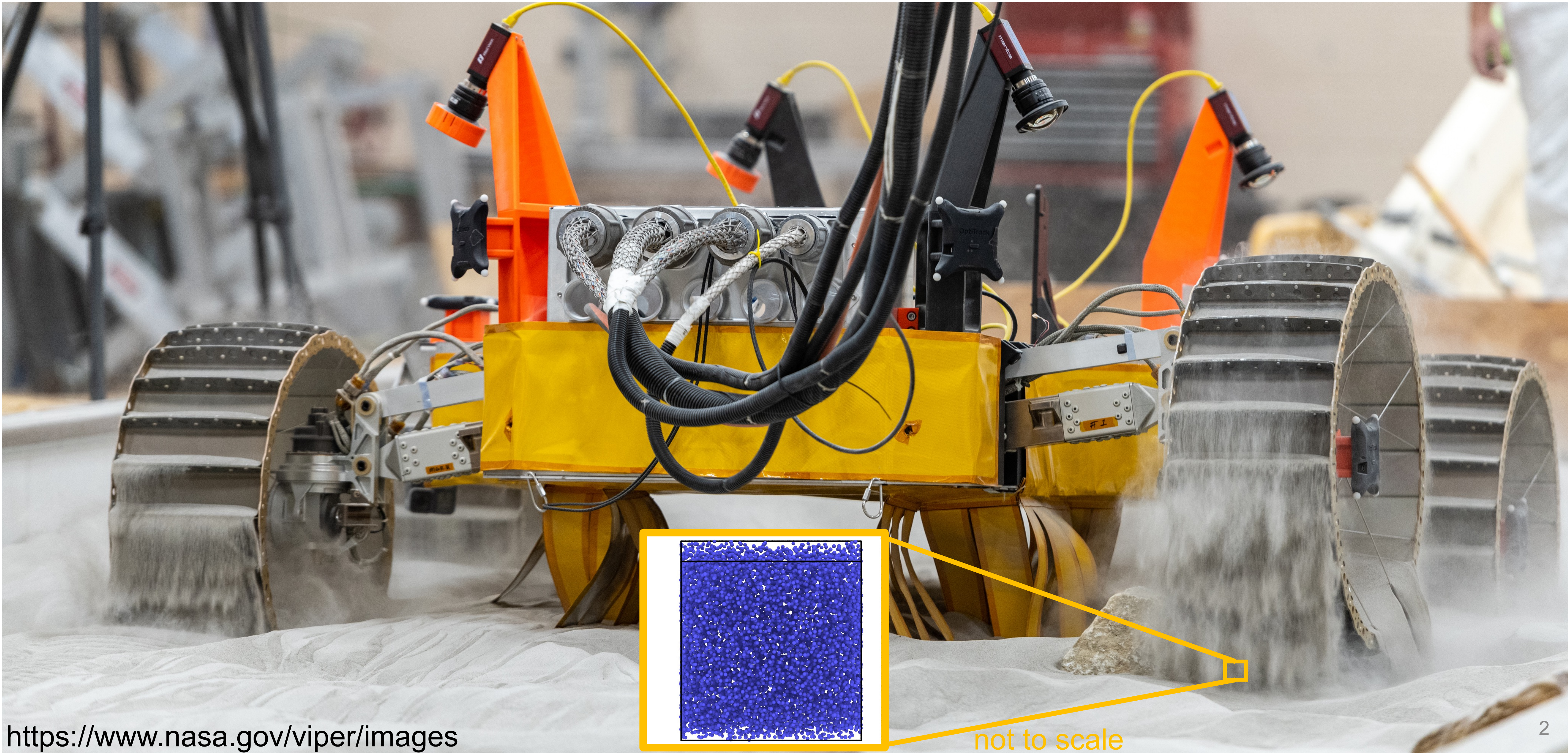

https://www.nasa.gov/viper/images

In-space manufacturing

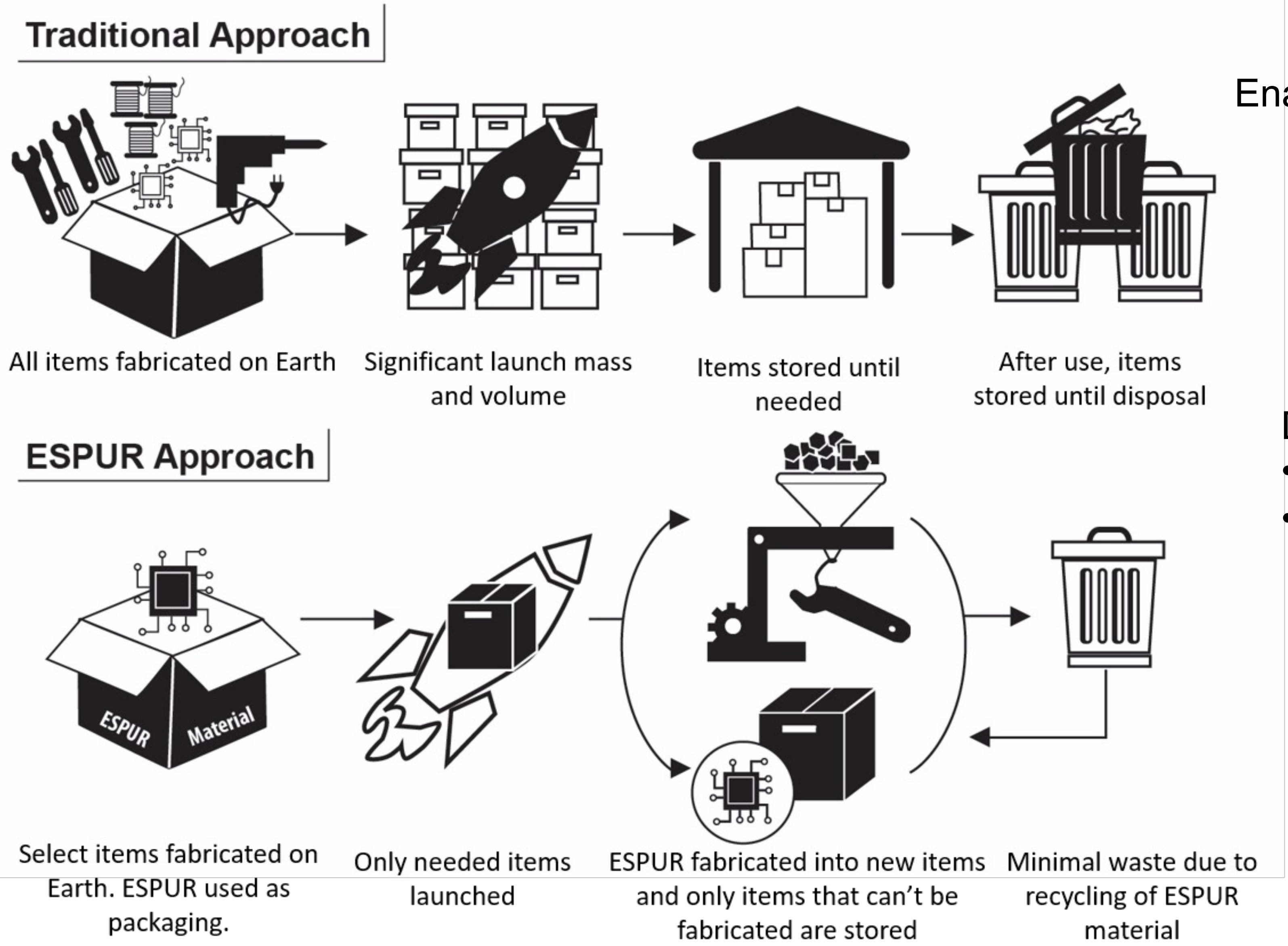

Microparticle modelling for Enabling Sustained Presence Using Recyclables (**ESPUR**)

Design desirables:

- Printed part strength
- Reversibility

Reversible Click Chemistry

Questions:

- How long does it take the Furan (A) and Maleimide (B) to find each other?
  - molecular weight
  - grafting density
  - entanglement length
- How can we improve strength by tuning:
  - Particle sizes
  - Particle shape
  - Interactions (friction, cohesion, elasto-plasticity)

Maleimide-furan reaction

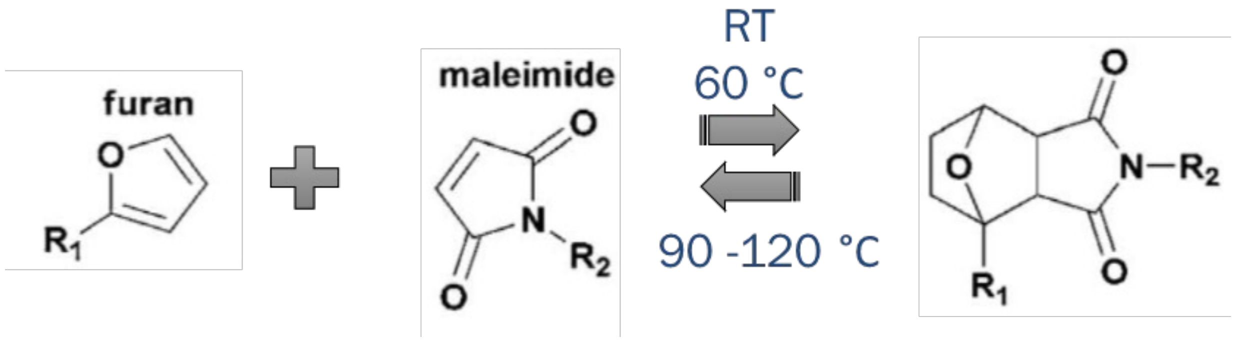

Prog. Polym. Sci. 2013, 38, 1-29.

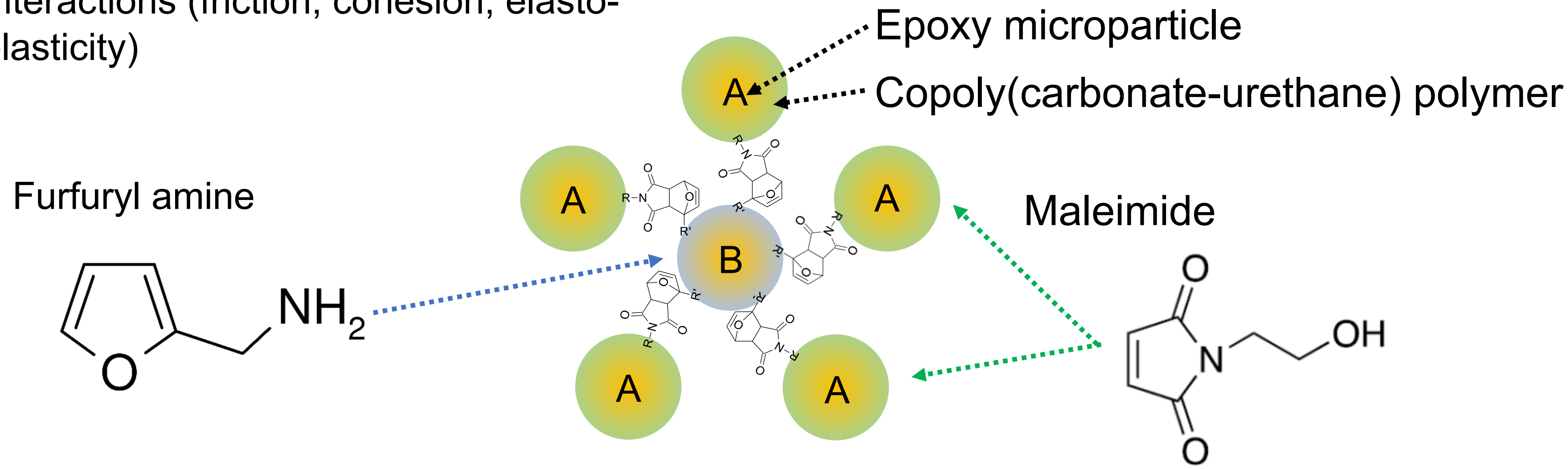

B. Zhang, et. al., Polym. Chem., 2015,6, 7368-7372

Modeling the polymer-grafted microparticles

Polymer physics modeling

Molecular dynamics (MD) with atomistic and coarse-grained models

Measure dynamics, structure and interactions

Microparticle modeling

Discrete element modeling (DEM) with particle models

Contact mechanics define particle-particle interactions

Measure microstructure and mechanical properties

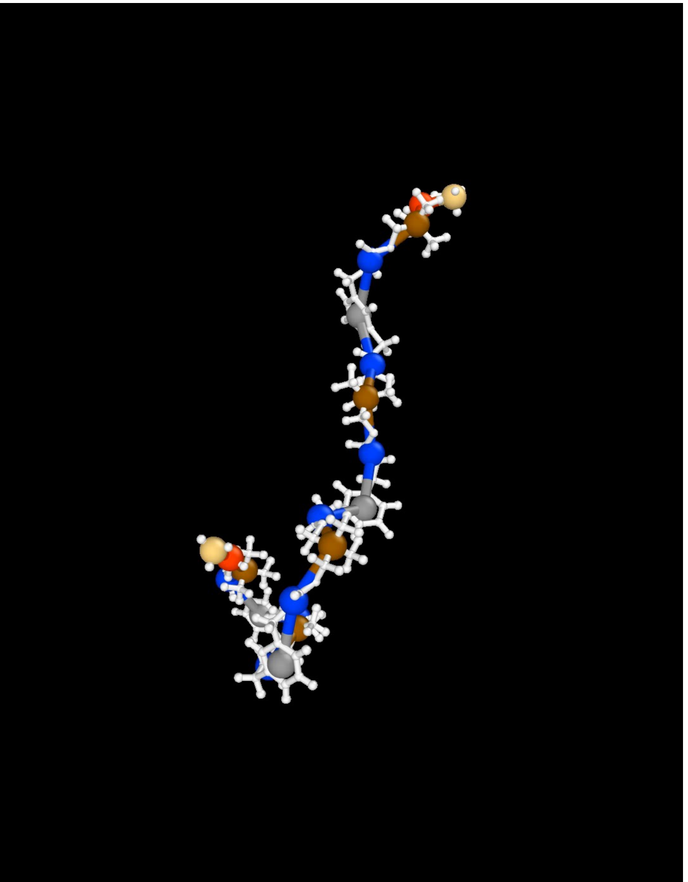

Lauren Abbott

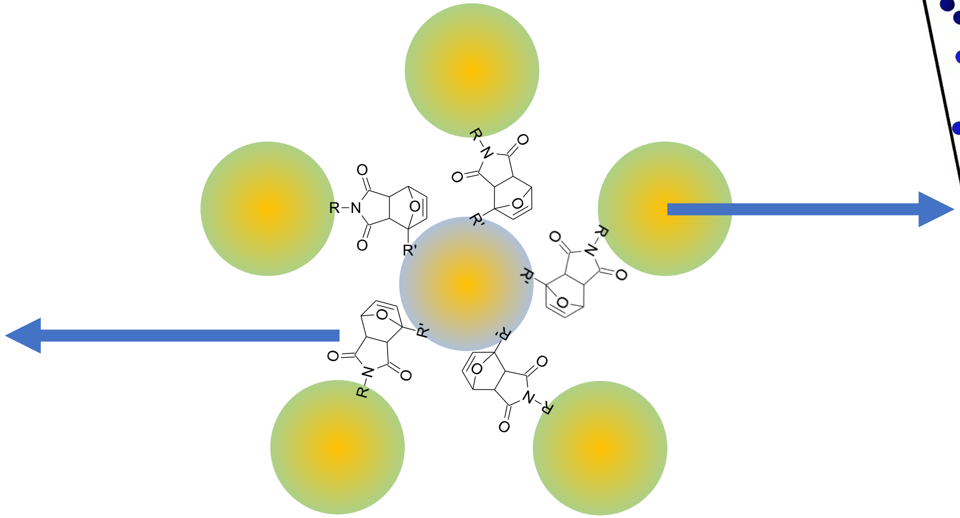

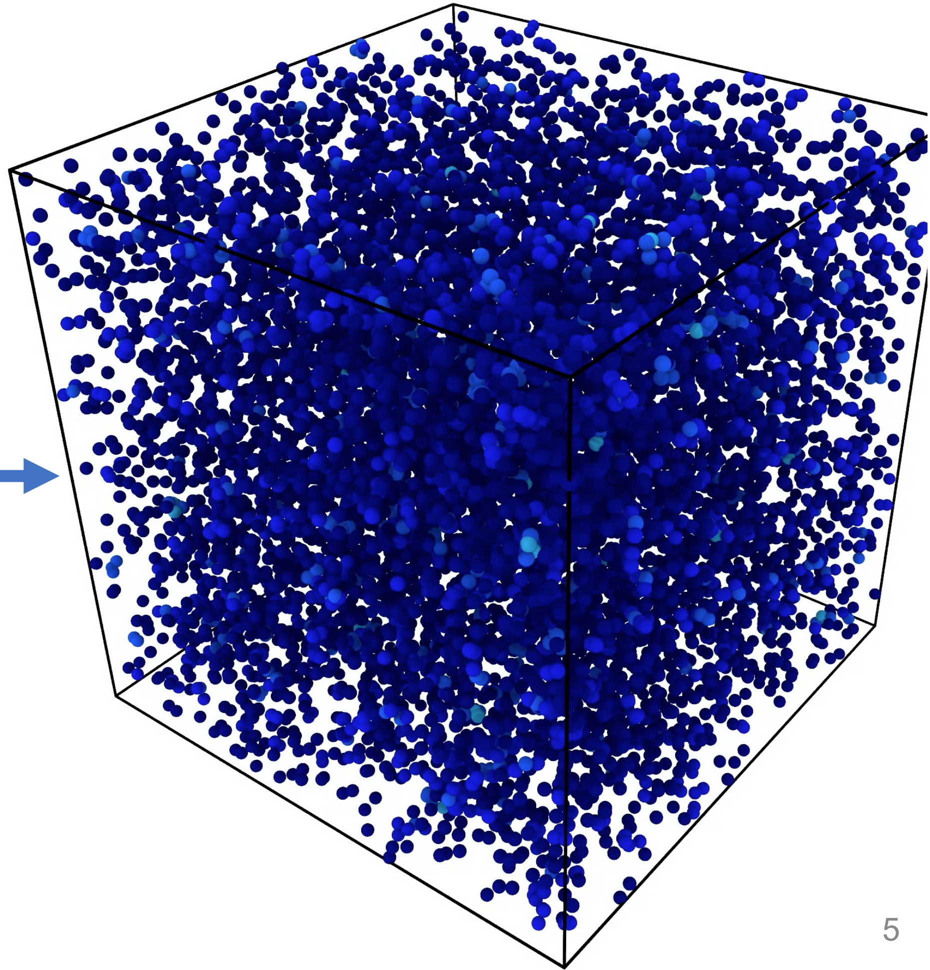

Connections with experiments

Brush/coating synthesis

Processing

Goal: Maximize number of A-B contacts ($N^{\text{contacts}} \approx$ Mechanical strength)

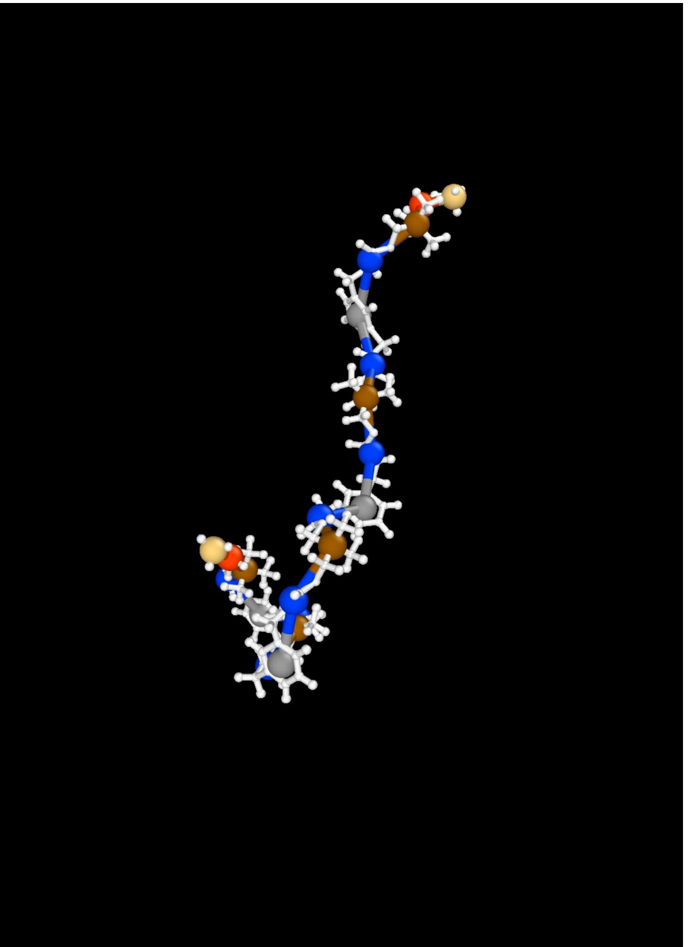

Atomic force microscopy

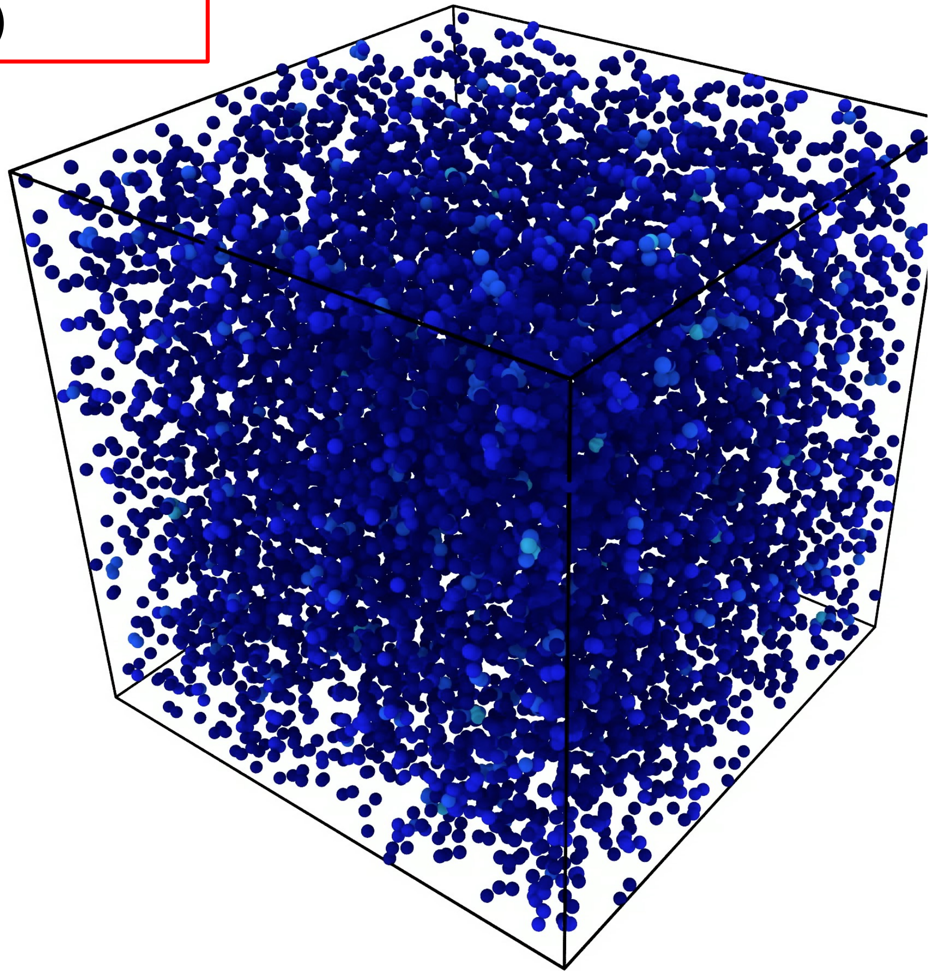

Microparticle methodology

Microparticle modeling
Discrete element modeling (DEM) with particle models
Hertzian and JKR contacts

- Packing protocol: specify pressure tensor and bring system to final state from a very low pressure.
- Dilute initial configuration (25% volume fraction)
- At least 1000 particles each of type A and B (up to 10 million total particles)

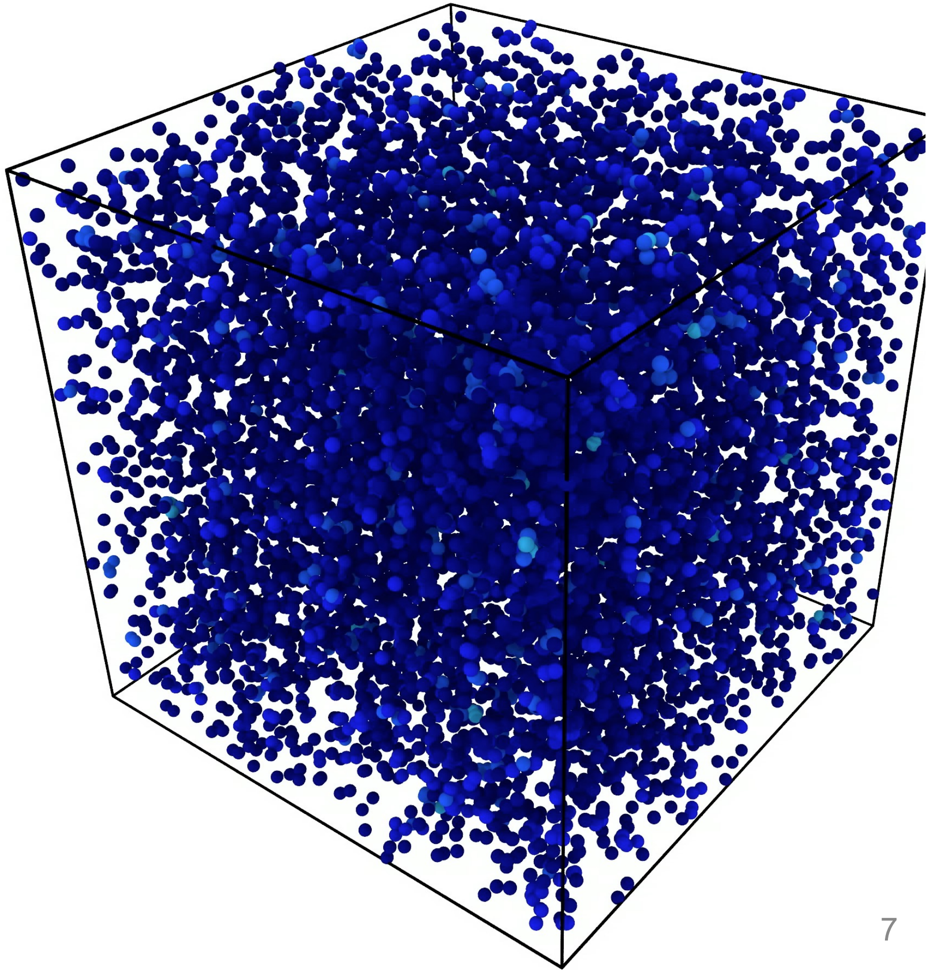

Plimpton S. (1995). *J. Comput. Phys.*, 117, 1-19.
Mindlin, R. D. (1949). *J. Appl. Mech., ASME* 16, 259-268.
Luding, S. (2008). *Granular matter*, 10(4), 235.

Particle design space

Size dispersity

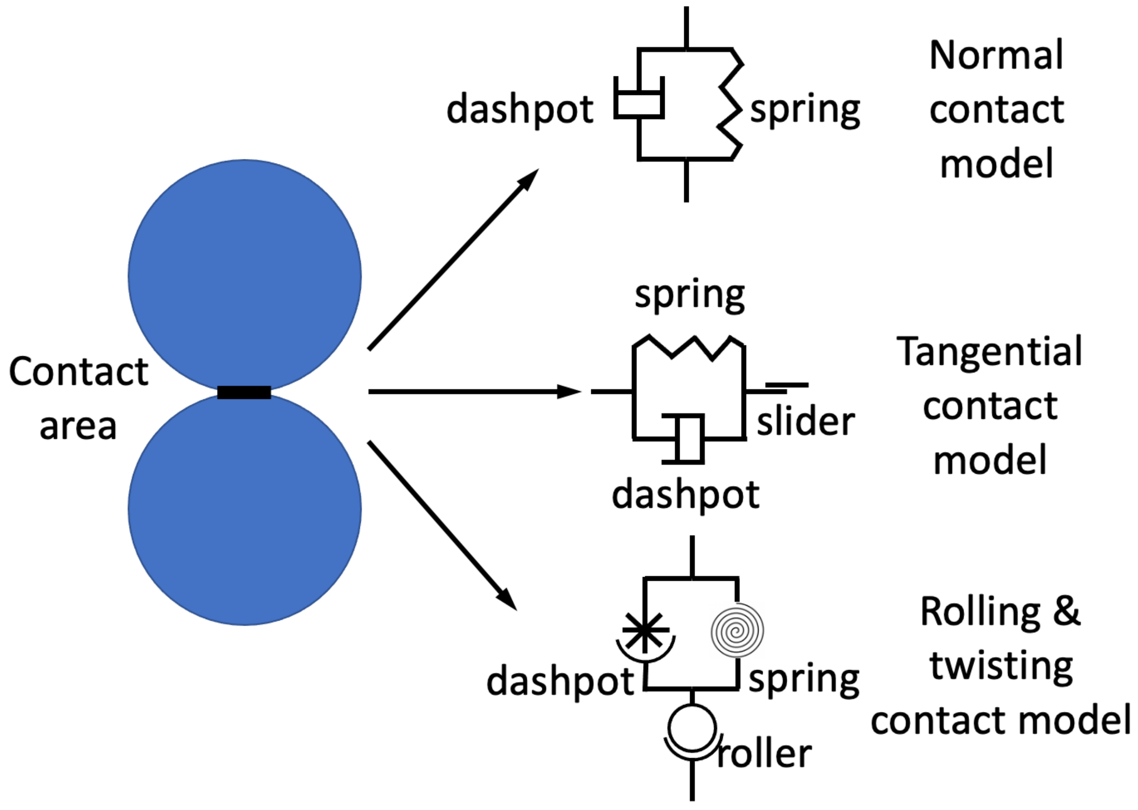

Interaction

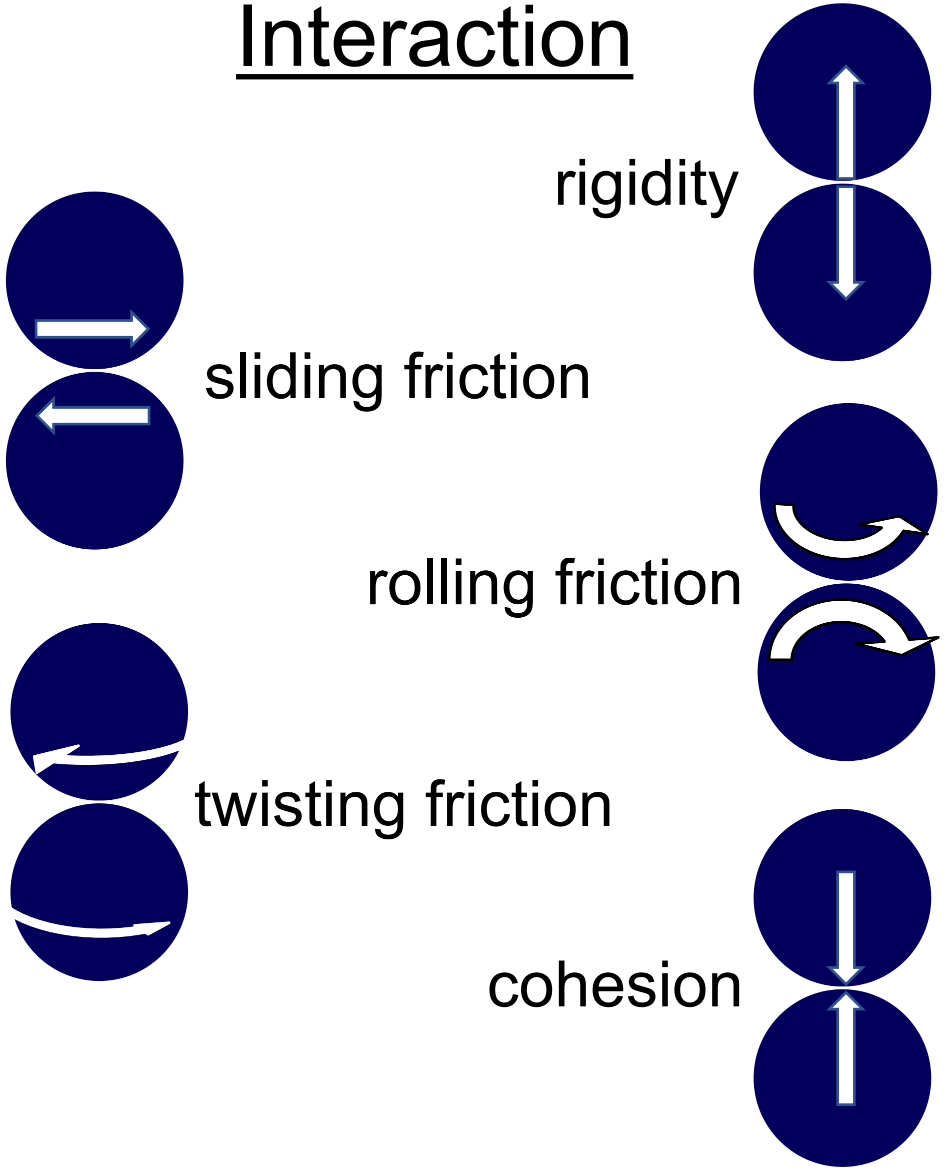

Contact mechanics model

Discrete element, particle-based modeling (DEM) (implemented within LAMMPS).

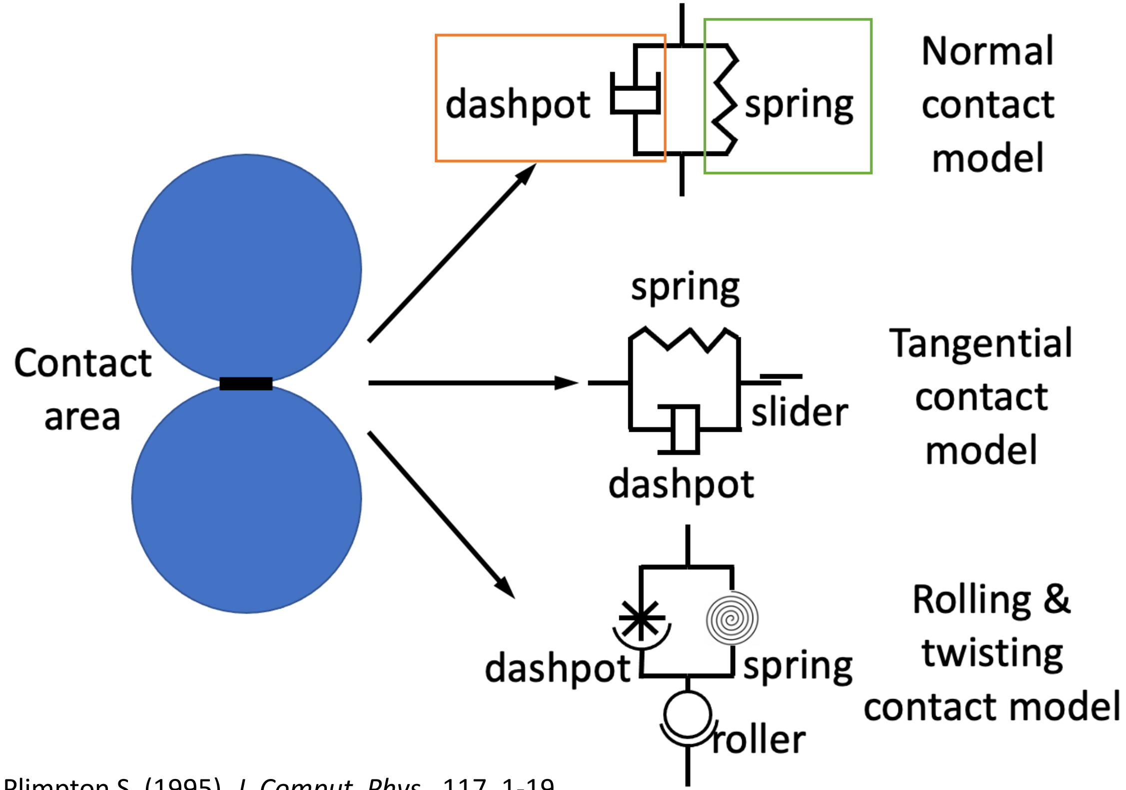

$$\mathbf{F}_{ne,Hertz} = k_n R_{eff}^{1/2} \delta_{ij}^{3/2} \mathbf{n}$$

$$\mathbf{F}_{n,damp} = -\eta_n \mathbf{v}_{n,rel} \qquad \eta_n = \eta_{n0}\, a m_{eff}$$

Property	parameter	model
Young's modulus	k_n	4.808 GPa
Poisson's ratio	k_s	
Coefficient of restitution	γ_n	0.009404 μm^{-1} ns^{-1}
density	mass	1.1 pg/μm^3
diameter		10 μm

Plimpton S. (1995). *J. Comput. Phys.*, 117, 1-19.
Mindlin, R. D. (1949). *J. Appl. Mech., ASME* 16, 259-268.
Luding, S. (2008). *Granular matter*, 10(4), 235.

Mono- and gaussian-dispersed simulations

Monodisperse simulations

Packing fraction:

$$\phi = \frac{V_{\text{particles}}}{V_{\text{box}}}, \phi_{\text{mono}} = 0.638$$

Coordination number:

$$Z = \frac{N^{\text{contacts}}}{N^{\text{particles}}} = Z_{\text{mono}} = 5.79$$

$$Zab = \frac{N_{ab}^{\text{contacts}} + N_{ba}^{\text{contacts}}}{N_{\text{total}}^{\text{particles}}}$$

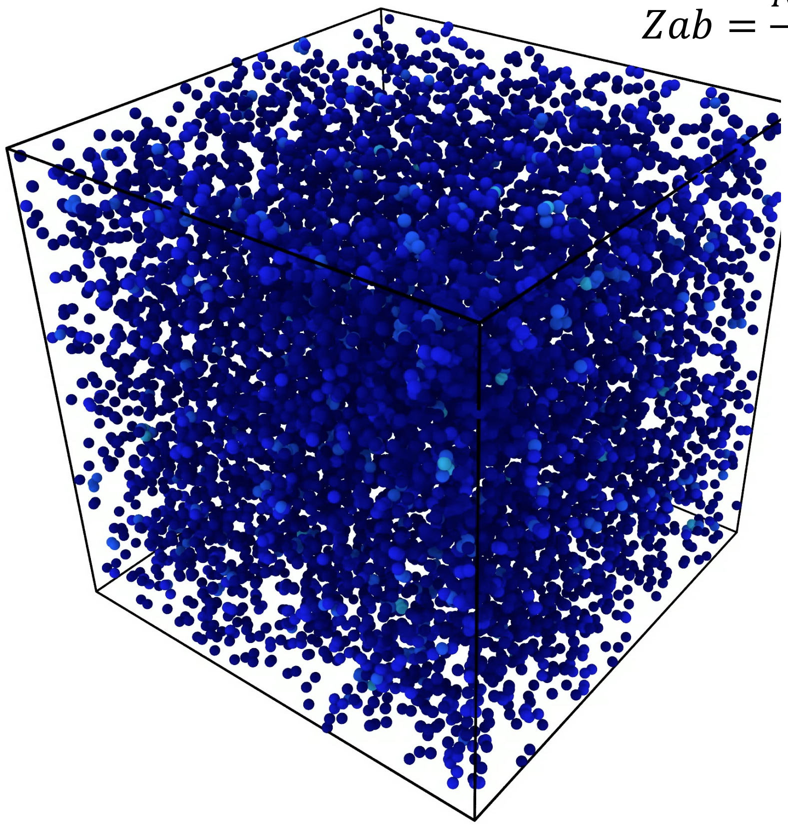

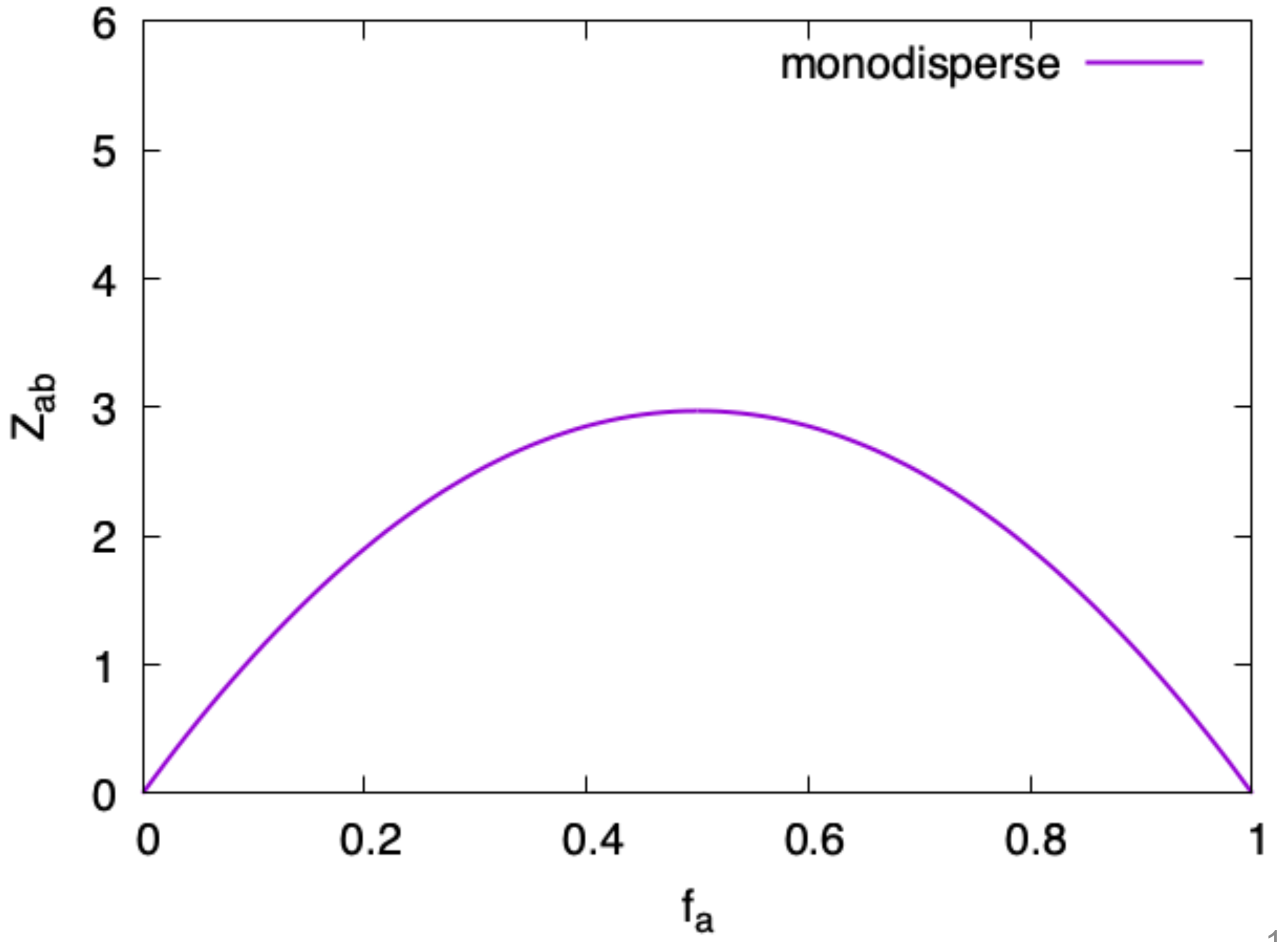

Polydisperse simulations

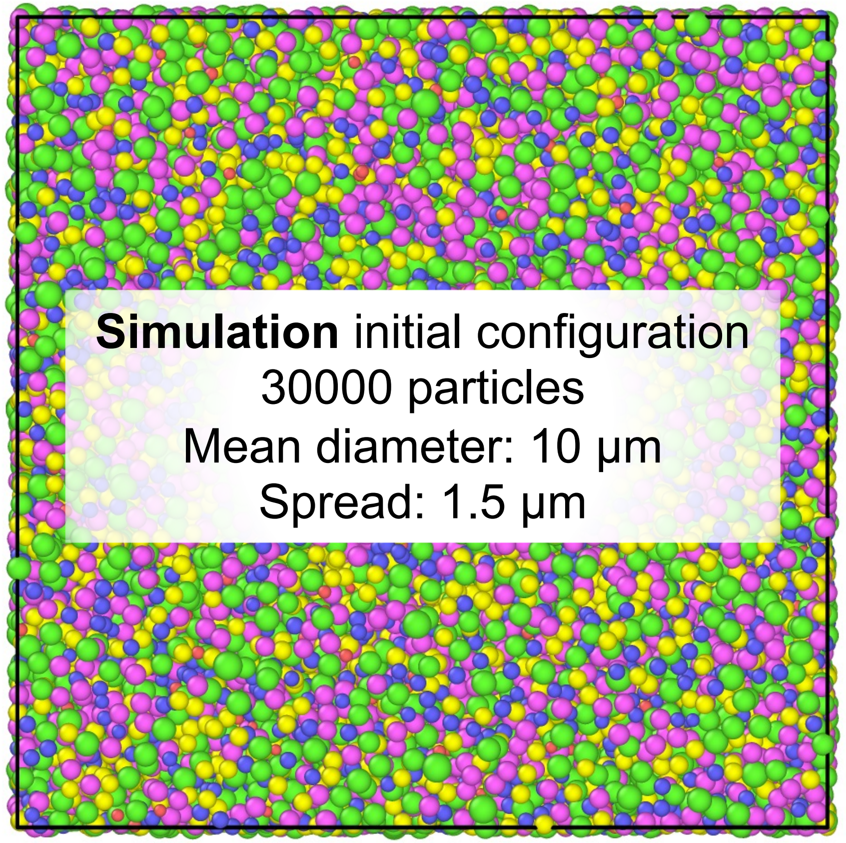

Experimental particle size distribution
Points: data
Line: fit

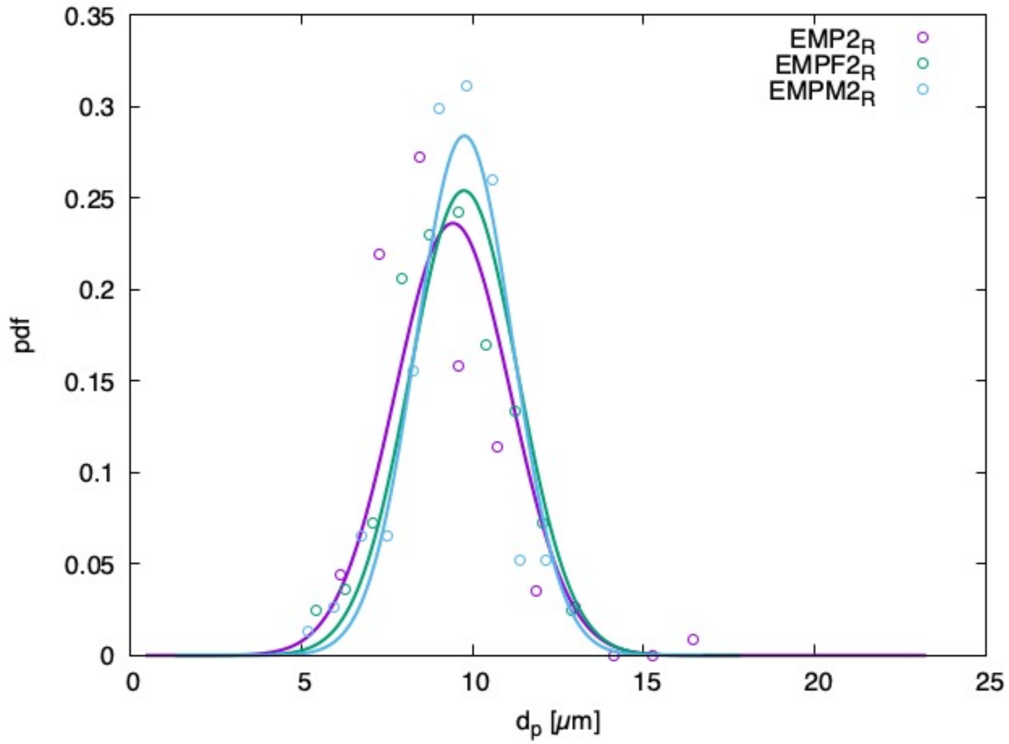

A-B coordination number increases with A-B fraction

Packing fraction:

$$\phi = \frac{V_{\text{particles}}}{V_{\text{box}}}, \phi_{\text{mono}} = 0.638\ \phi_{\text{gauss}} = 0.648$$

Coordination number:

$$Z = \frac{N^{\text{contacts}}}{N^{\text{particles}}} = Z_{\text{mono}} = 5.79\ Z_{\text{gauss}} = 5.66$$

$$Zab = \frac{N_{ab}^{\text{contacts}} + N_{ba}^{\text{contacts}}}{N_{\text{total}}^{\text{particles}}}$$

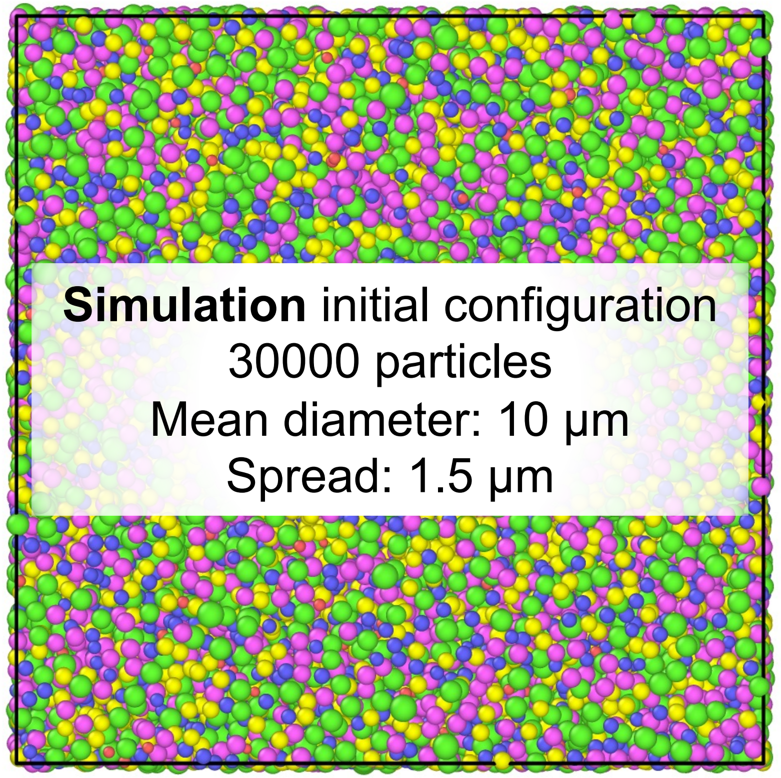

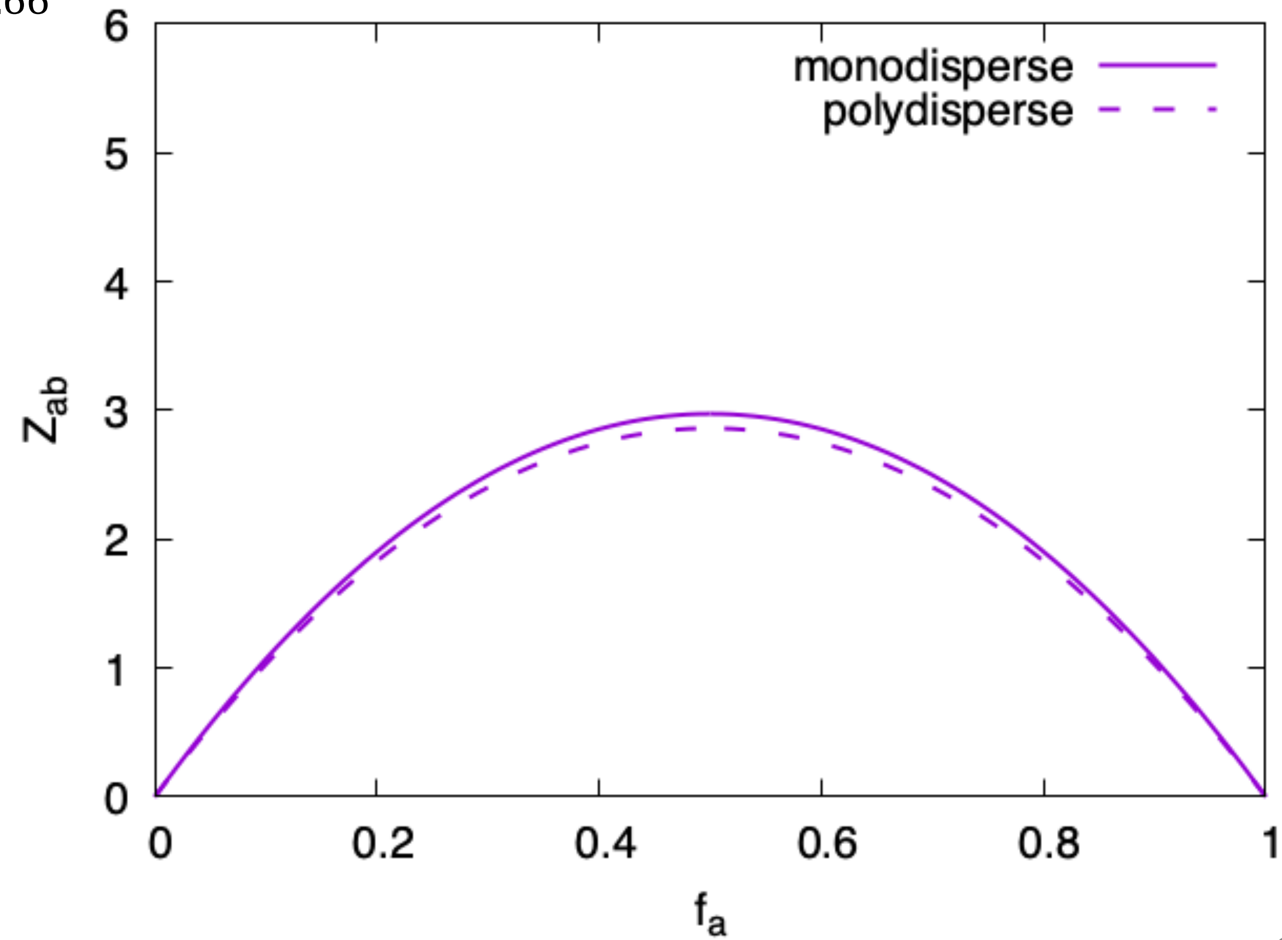

Bidisperse simulations dispersity range

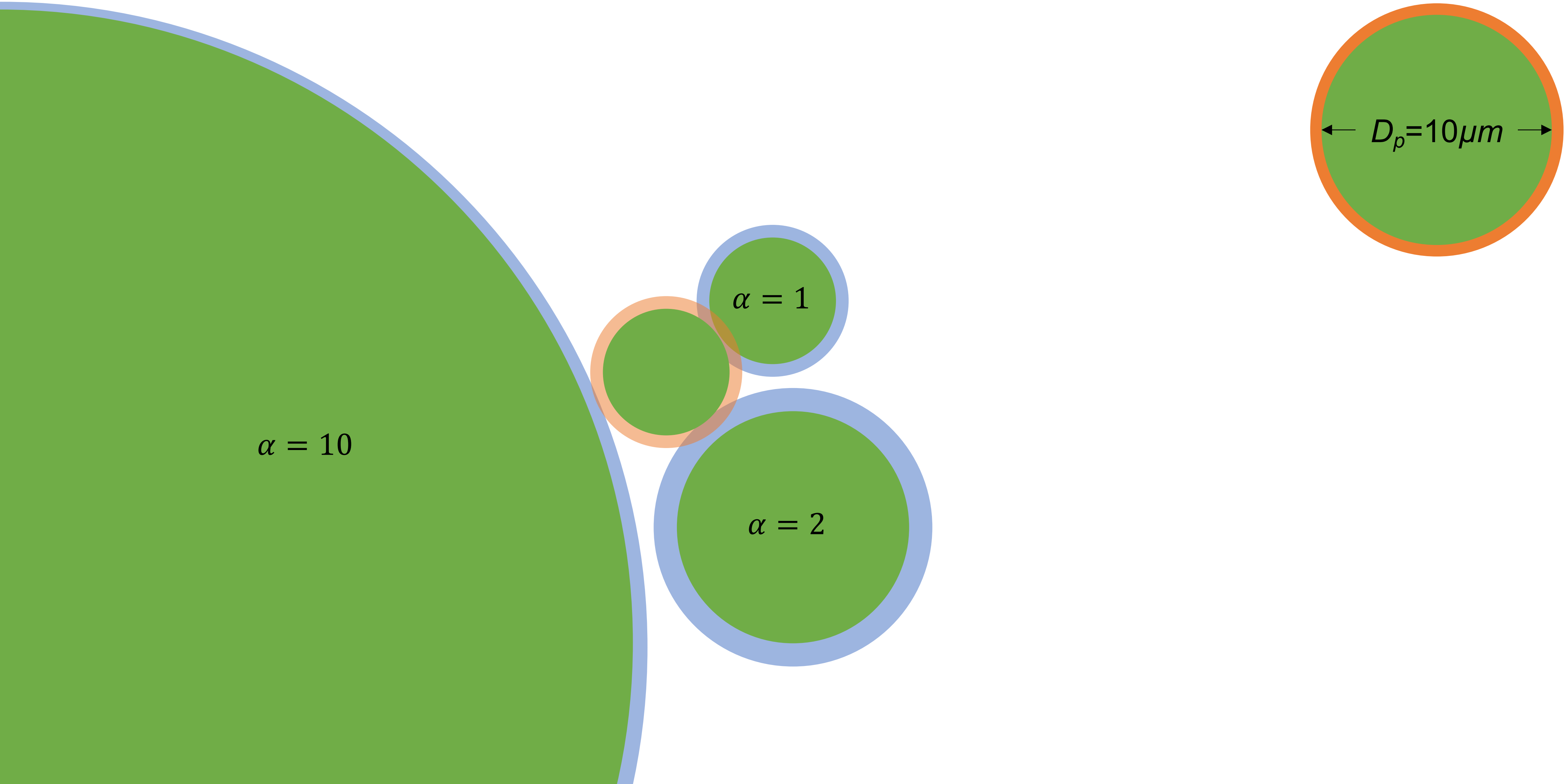

Volume fraction increases with dispersity

$$\alpha = \frac{D_b}{D_a} = \frac{D_{large}}{D_{small}}$$

$$f_a = \frac{\phi_{small}}{\phi_{small} + \phi_{large}} = \frac{N_{small}}{N_{small} + N_{large}\alpha^3}$$

$$\phi = \frac{V_{particles}}{V_{box}} = \frac{\frac{\pi}{6}\left(N_{small}{D_{small}}^3 + N_{large}{D_{large}}^3\right)}{V_{box}}$$

- Agreement with previous results
  - Shows hertzian and hookean have similar bidisperse packing behavior
- Larger size ratio -> lower void fraction -> more strength

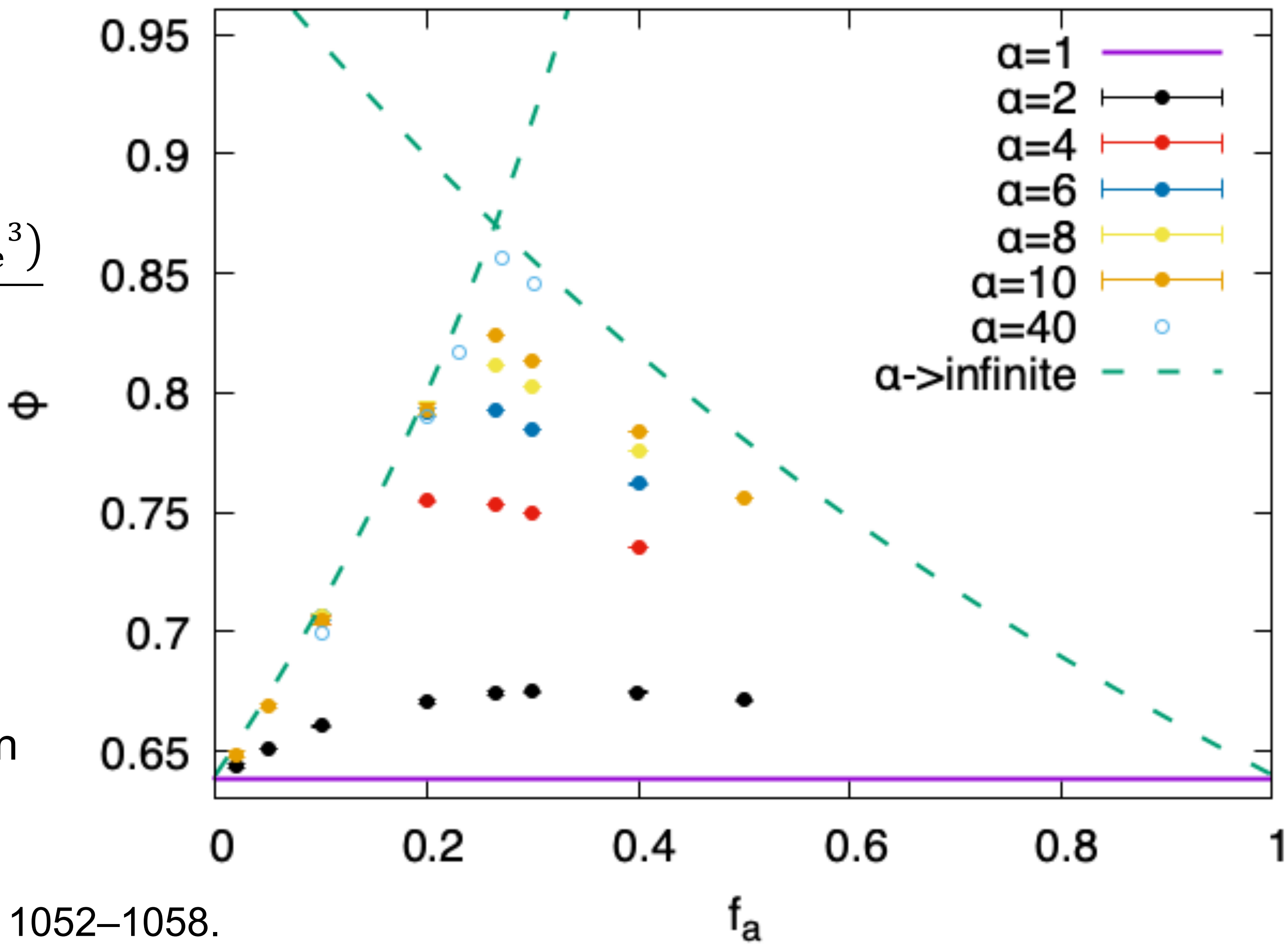

Furnas, C. C. *Ind. Eng. Chem.* **1931**, *23* (9), 1052–1058.
Srivastava, I. *et al*. *Phys. Rev. Research* **2021**, *3* (3), L032042.

Small-large coordination number decreases with α

$$Zab = \frac{N_{ab}^{\text{contacts}} + N_{ba}^{\text{contacts}}}{N_{total}^{\text{particles}}}$$

- Many smalls are rattlers for large α
- **Smaller** size ratio -> more contacts -> more strength
- Different story than some theory

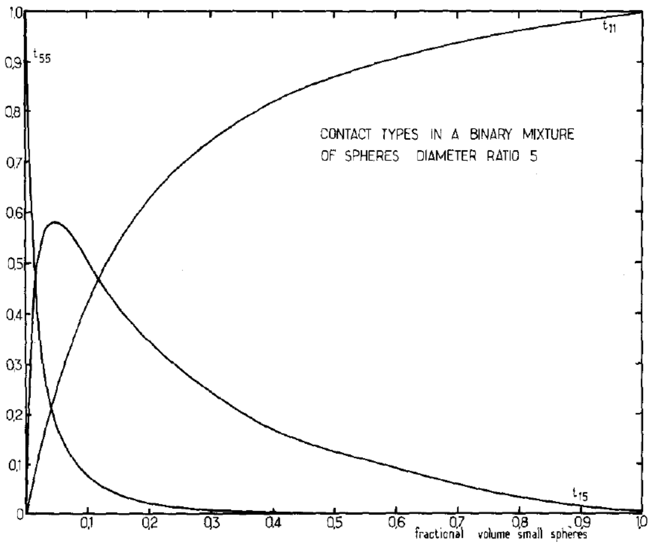

FIG. 5. Contact types in a binary mixture of spheres diameter ratio 5.

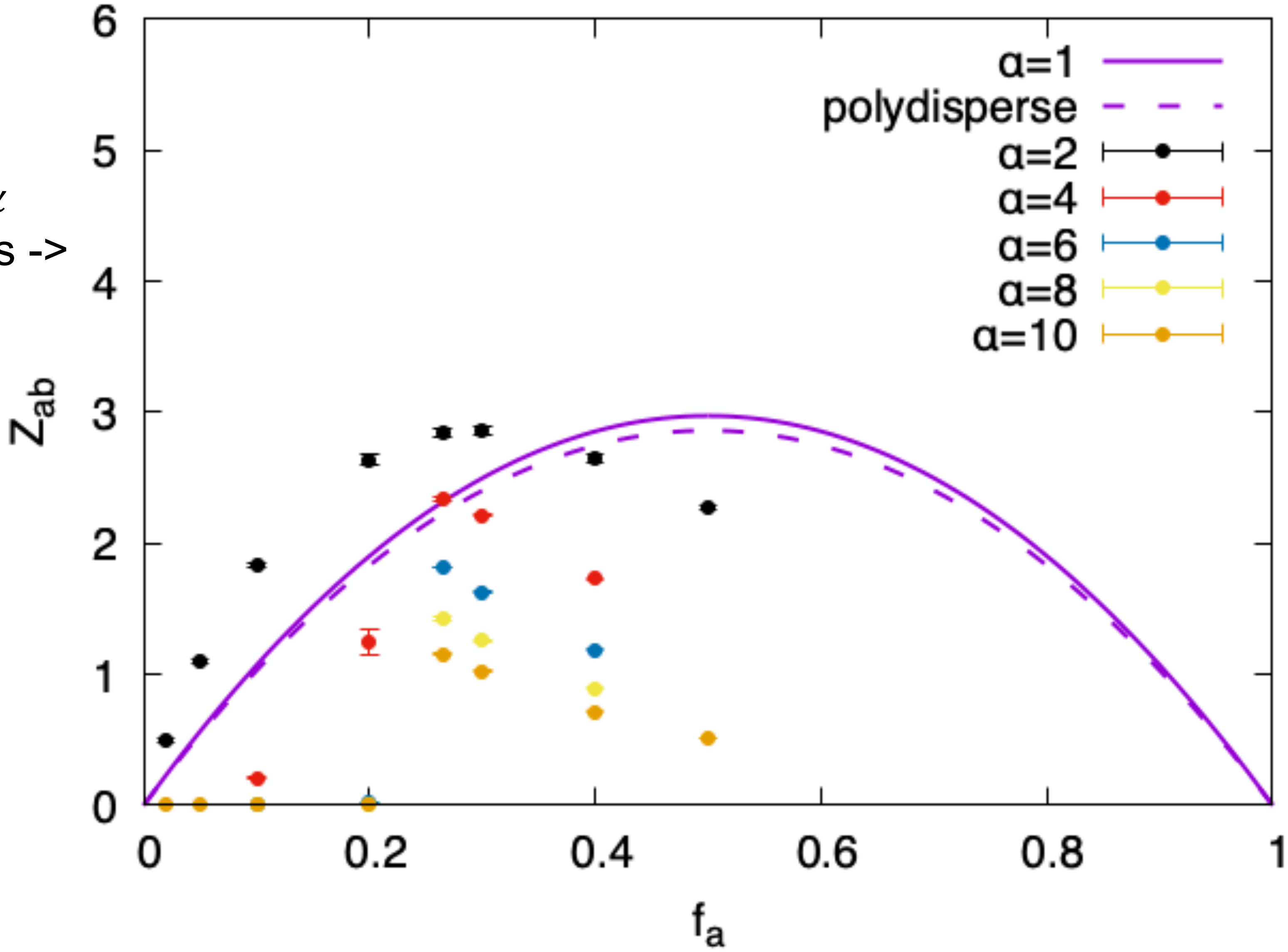

Dodds, J. A. *Journal of Colloid and Interface Science* **1980**, *77* (2), 317–327.

Peak density, peak contacts and other conclusions

- Monodisperse to weakly polydisperse causes increased density but decreased A-B contacts
- 50% vol A is the optimal mixture for mono and polydisperse particle sizes
- The peak volume fraction corresponds with a peak in A-B contacts for bidisperse packings.
- Increasing size ratio causes the volume fraction to increase and A-B contacts to decrease.

Acknowledgments

Lauren Abbot[1], Samantha I. Applin[2,4], Miranda L. Beaudry[2], Alexander J. Blanchard[3], Bryce L. Horvath[2], Hannes Schniepp[4], Christopher J. Wohl[2]

[*]Analytical Mechanics Associates, Inc.
[1]NASA Ames Research Center
[2]NASA Langley Research Center
[3]NASA Marshall Space Flight Center
[4]William and Mary University

Rolling and Twisting friction

Rolling and twisting torque resistance sources

- Load asymmetry built up by:
  - microslip and creep
  - inelastic deformation at contact area
  - roughness

Rotational motion and friction in hopper

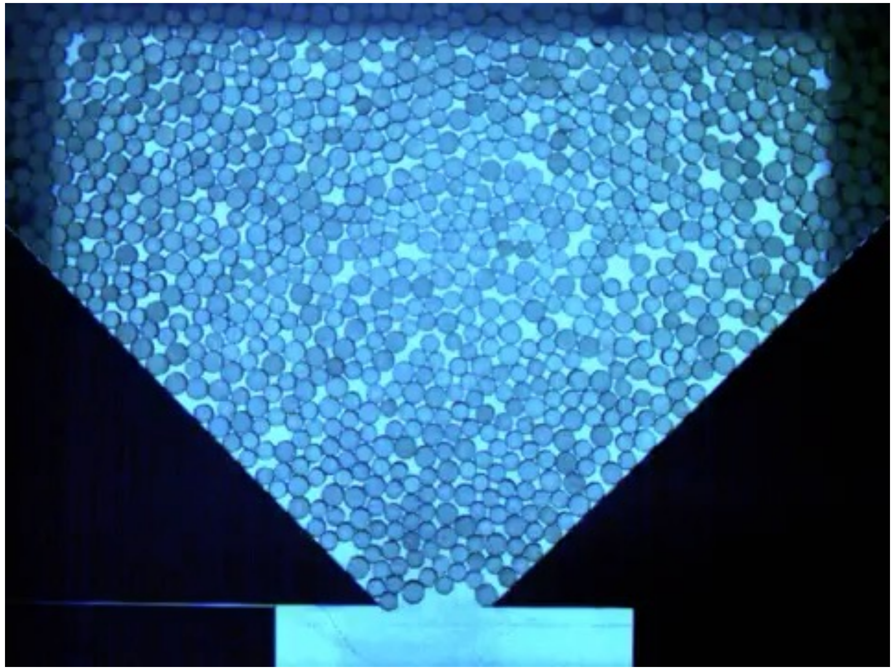

Tang and Behringer (2011). *Chaos,* 21, 041107

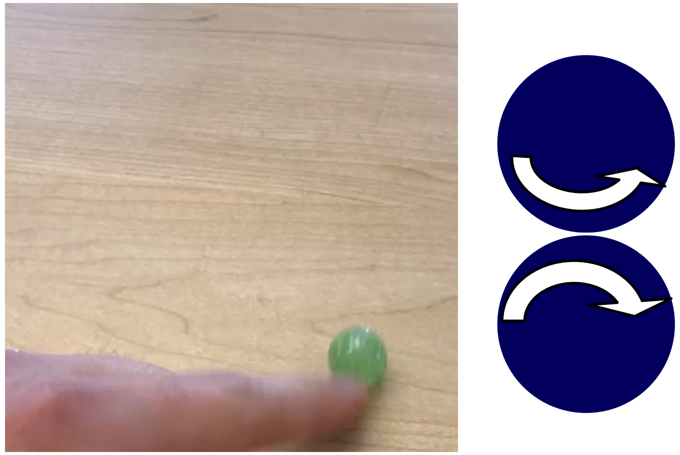

Rolling

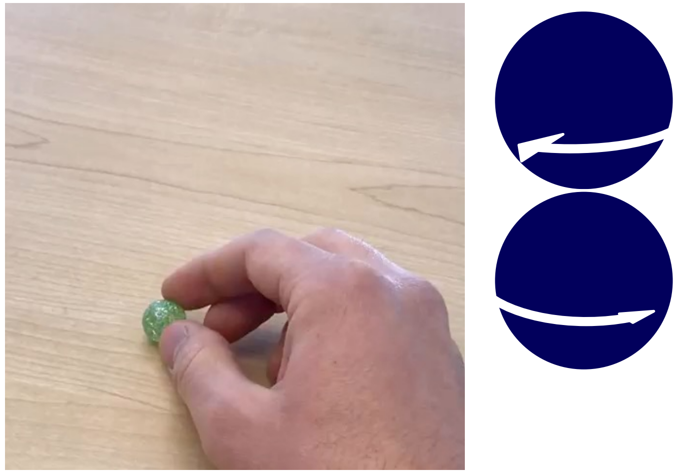

Twisting

Constraint counting

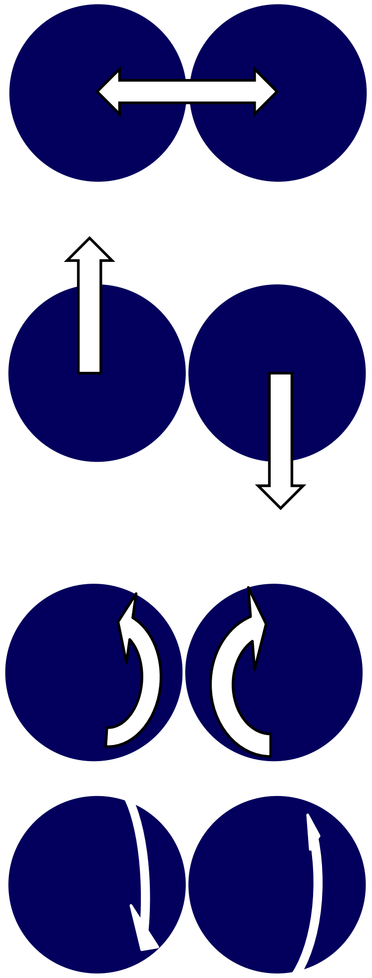

Theory for a stable packing:
The total number of constraints at contact are equal or greater than the total number of equations of motions

$$N^{\text{eqn}} = \begin{cases} 6N, \text{if 3d, frictional} \\ 3N, \text{if 2d, frictional} \\ 3N, \text{if 3d, frictionless} \\ 2N, \text{if 2d, frictionless} \end{cases}$$

$$N^{\text{eqn}} = \frac{N^c}{2} N \langle Z \rangle \quad \text{at jamming}$$

$$\langle Z \rangle = \frac{2N^{\text{eqn}}}{N^c N}$$

Avg. contacts/particle
"coordination number"

Friction	<Z>
frictionless	6
sliding friction	4
sliding + rolling + twisting friction	2

Microstructure and rattlers

$\mu_s=\mu_r=\mu_t=0$ $\mu_s=\mu_r=\mu_t=0.3$ $\mu_s=\mu_r=\mu_t=1$

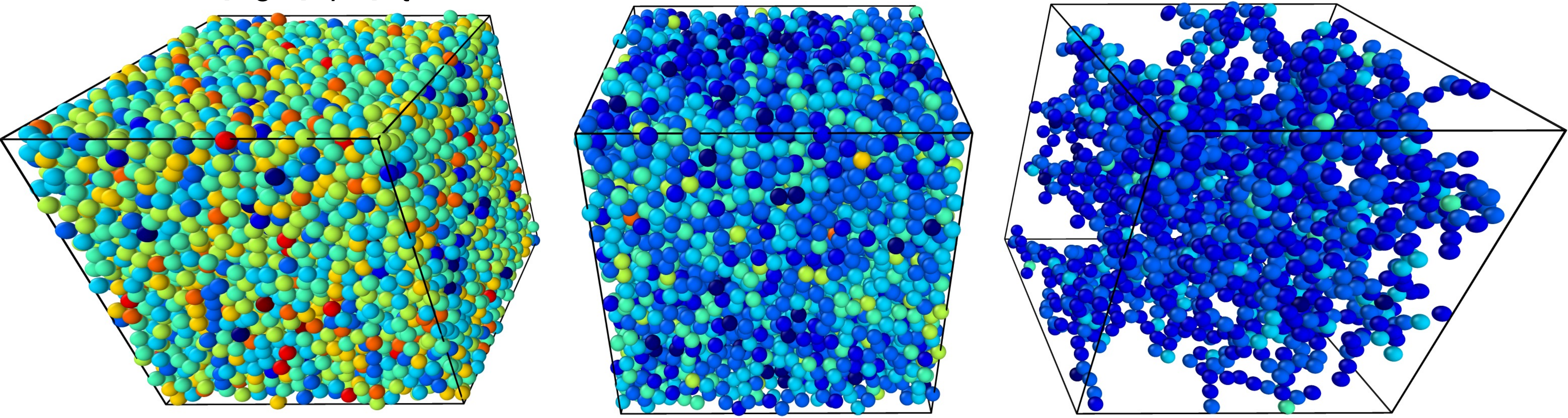

$$Z = \frac{\#\ of\ contacts}{particle}$$

Simulations vs theory - coordination

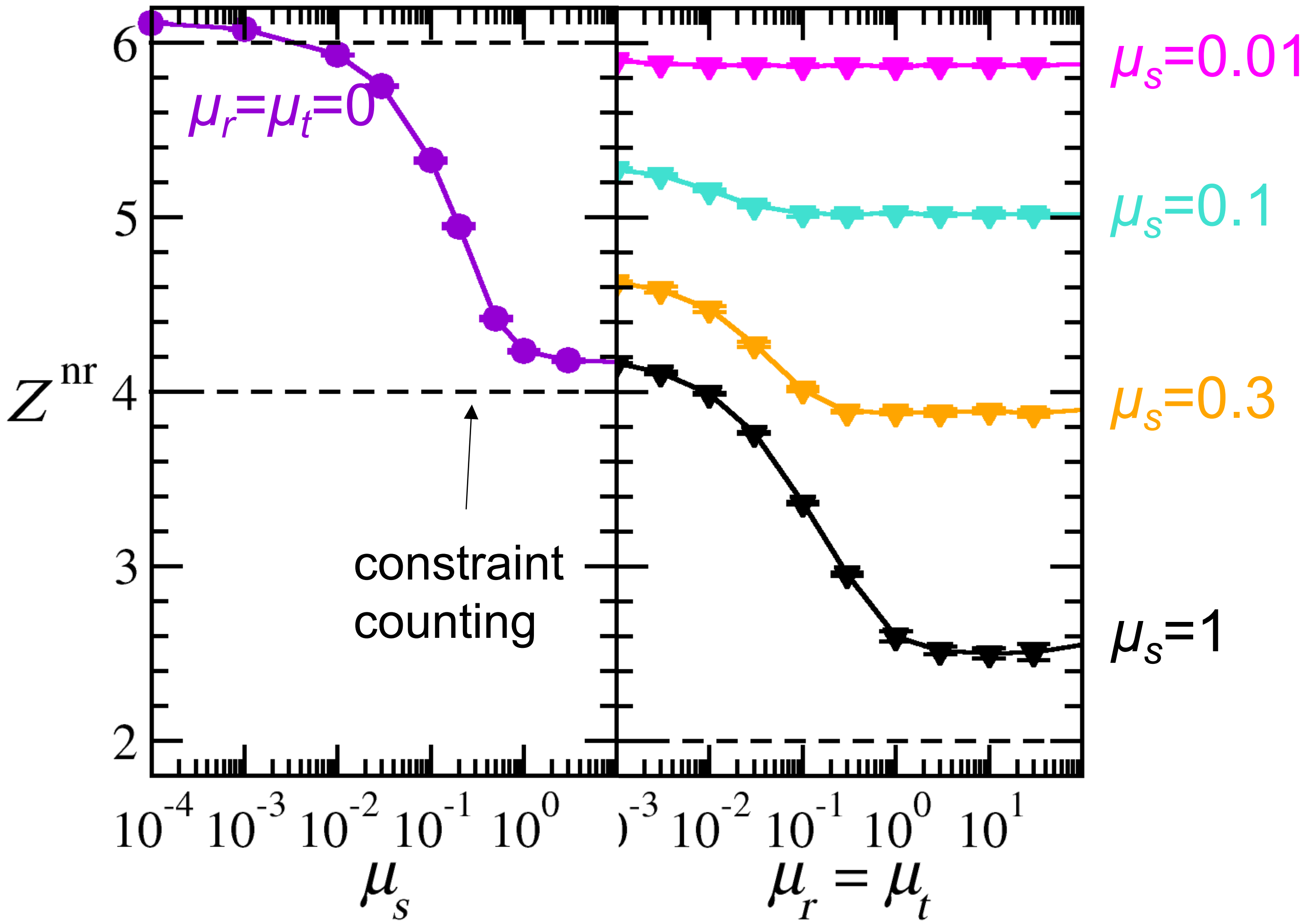

- Constraint counting under-predicts, but is affirmed by simulations
- min(Z^{nr}) ~ 2.45

Experimental comparison

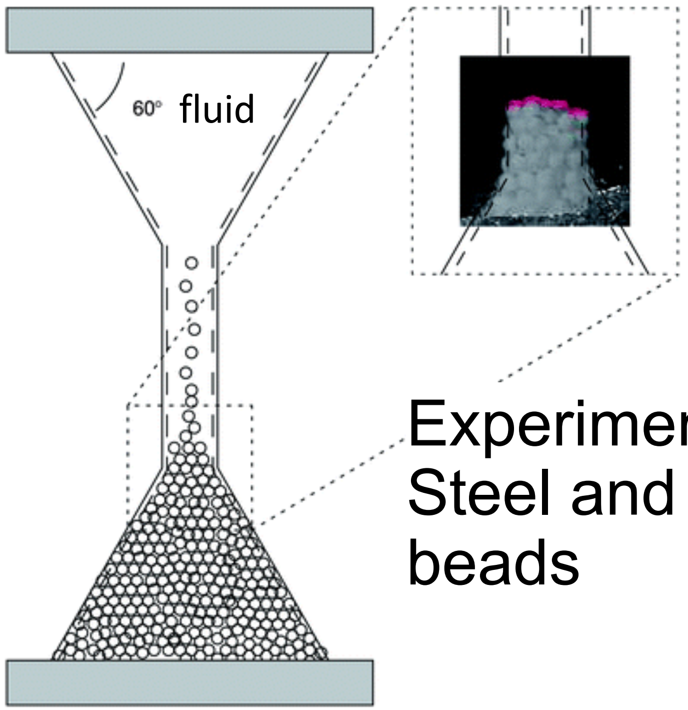

Experiments of Al, Steel and plastic beads

Menon N. et al. (2010). *Soft Matter*, 6(13), 2925-2930

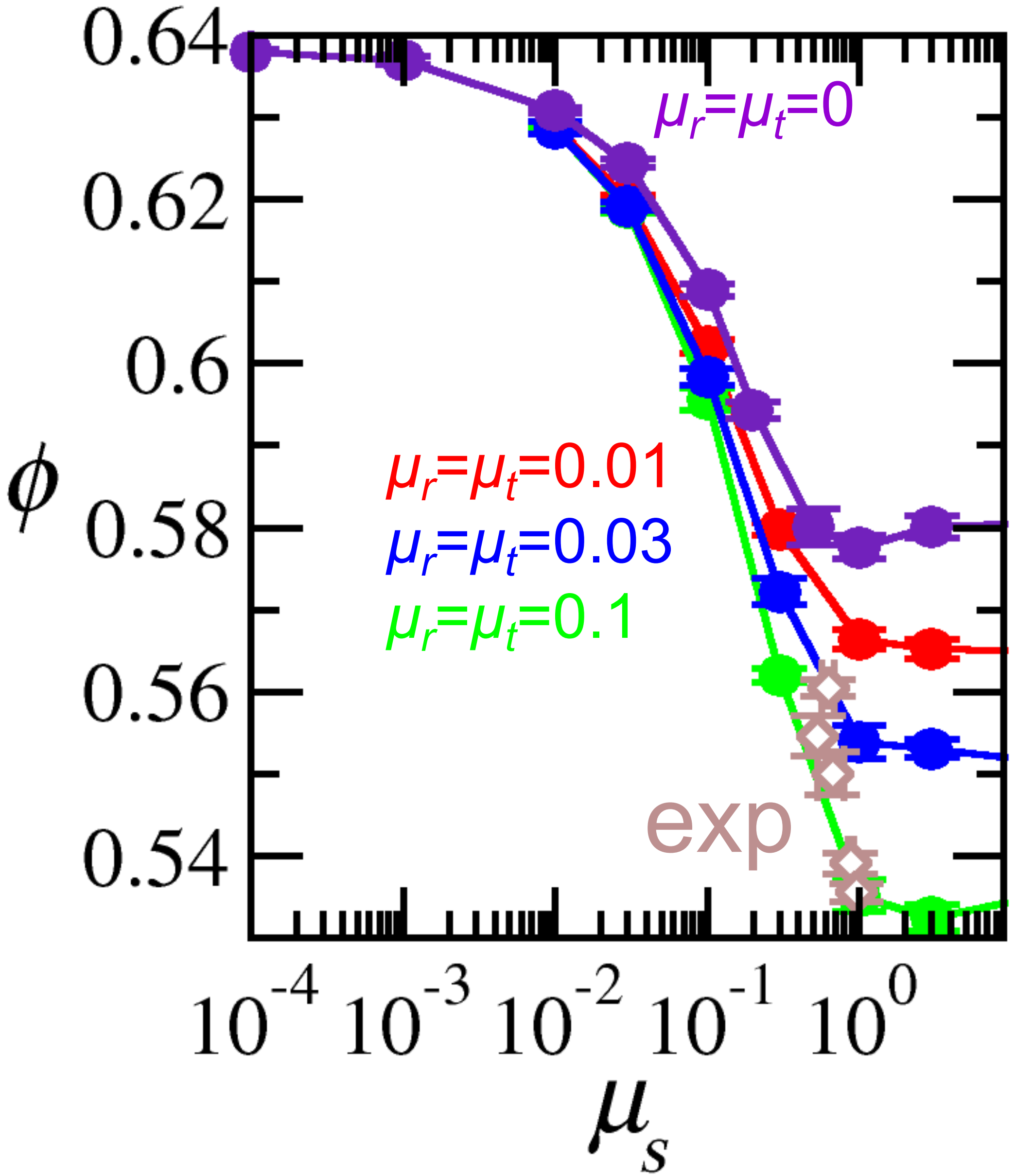

- Simulations agree with experiments with moderate rolling and twisting friction
- Rolling and twisting friction have little effect for low μ_s

Bidisperse packings

α: size ratio
f^s: smalls fraction

- Tractable simulations of huge size ratios (40:1) possible due to LAMMPS
- Limiting behavior is attained for ratios around 20:1

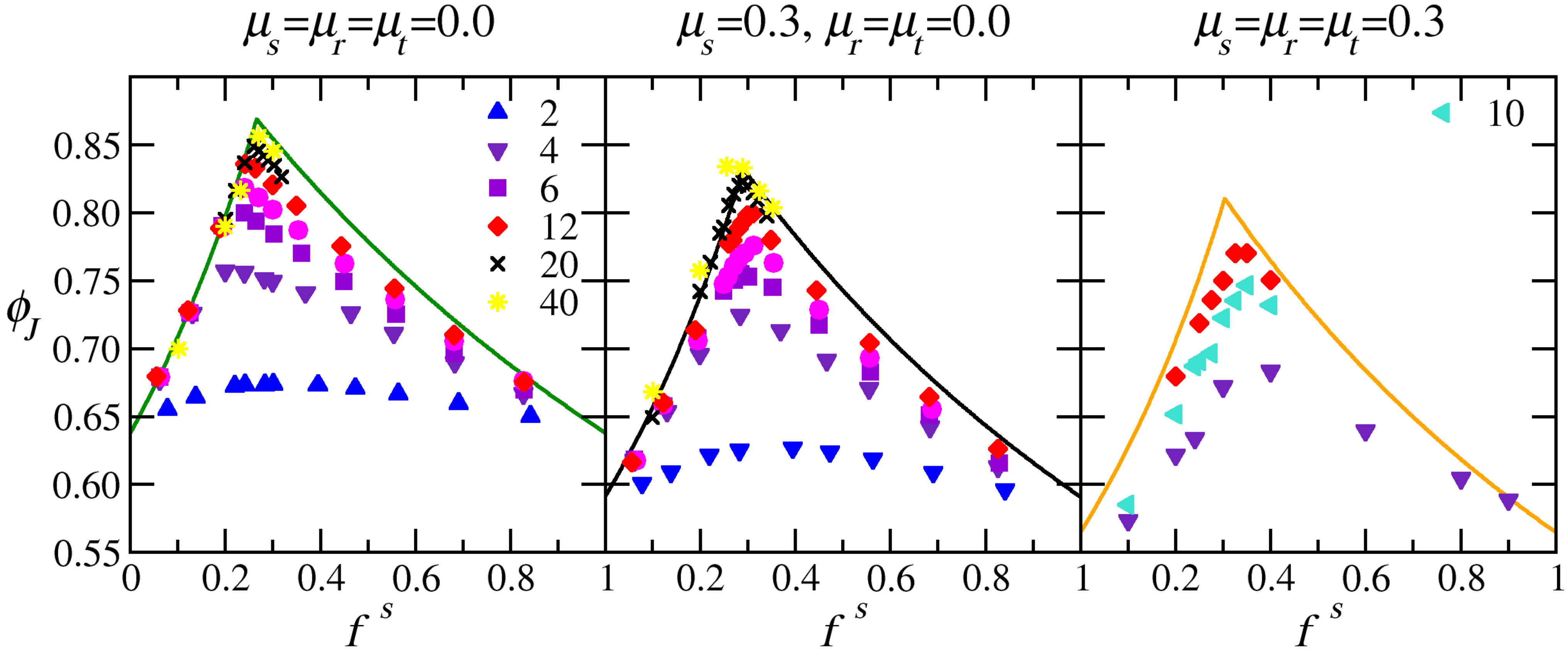

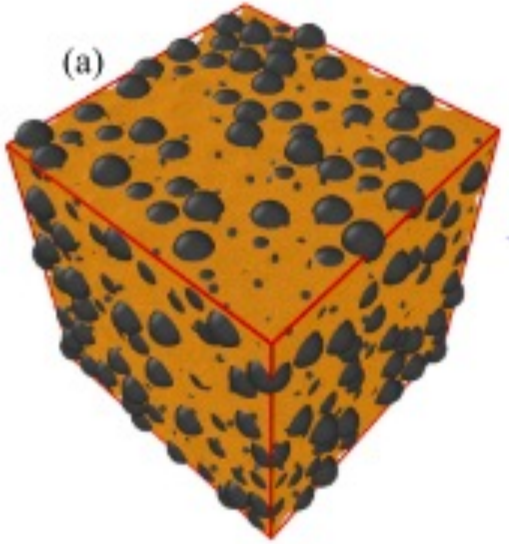

Srivastava, I., *et al.* (2021). *Physical Review Research*, *3*(3), L032042.

Conclusions

- <Z> goes from 6 to 2.5
- Agreement with experimental ϕ when $\mu_r \neq \mu_t \neq 0$
- Rolling and twisting friction cause large changes in microstructure
- Role of rolling and twisting friction on bidisperse packing is predicted by monodisperse packing

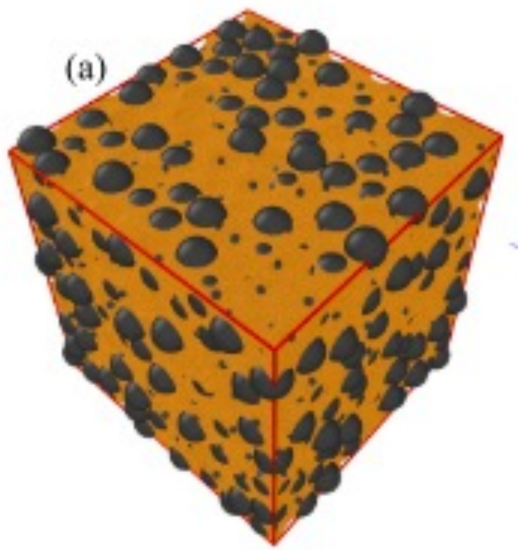

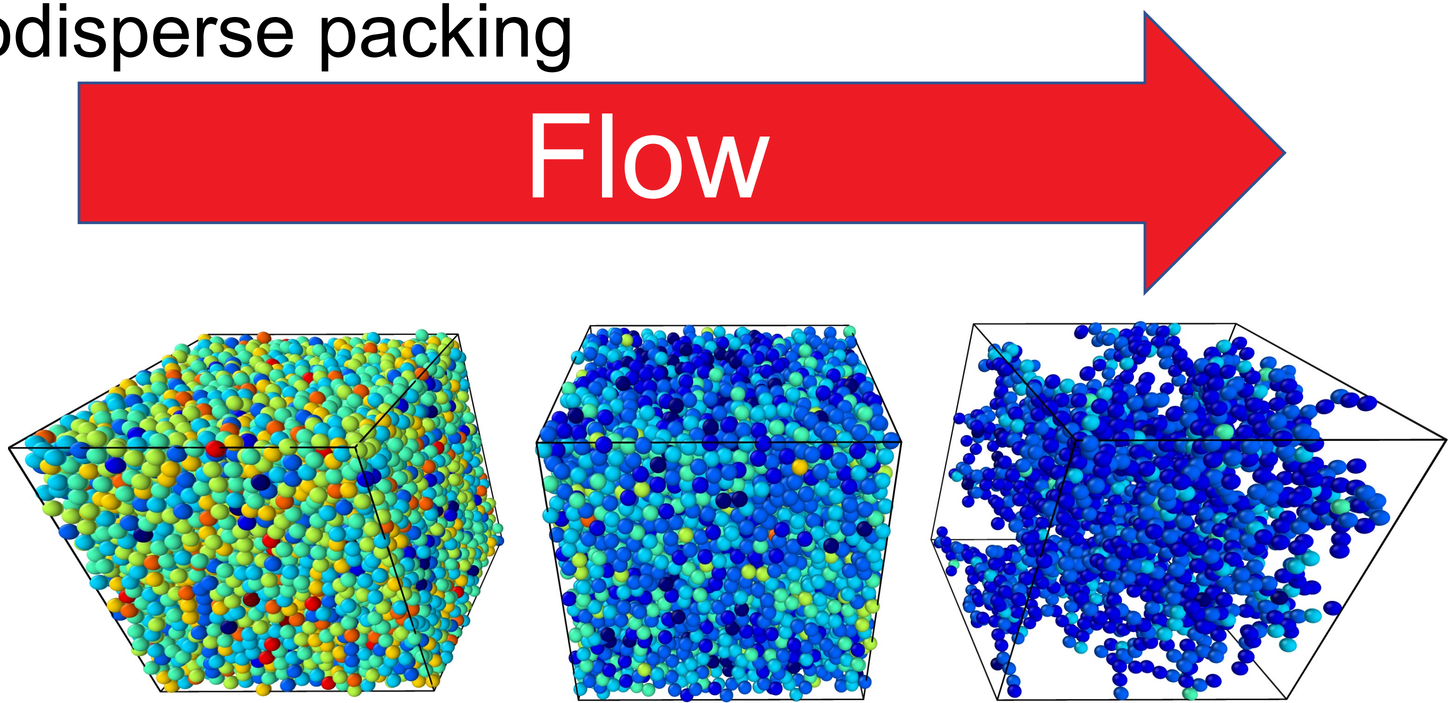

Predicting granular flow behavior

- Realistic modeling is necessary to match experimental systems because:
  - Rolling and twisting friction change microstructure and yield-stress
  - Size distributions is not monodisperse
- DEM simulations:
  - Can predicting flow behavior
  - Support constitutive law development
  - Experimental measurement interpretation

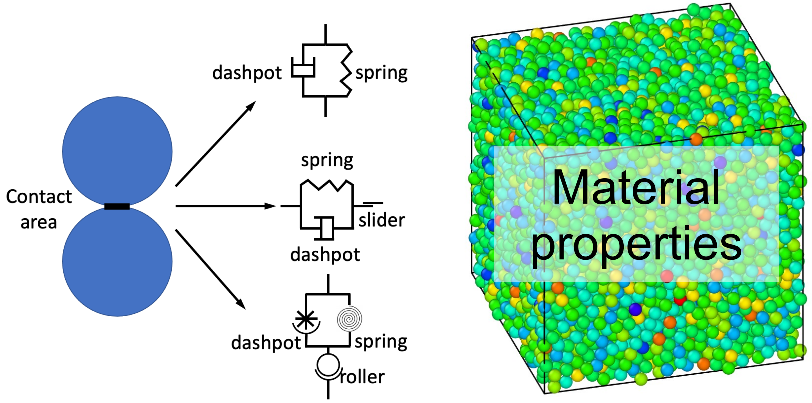

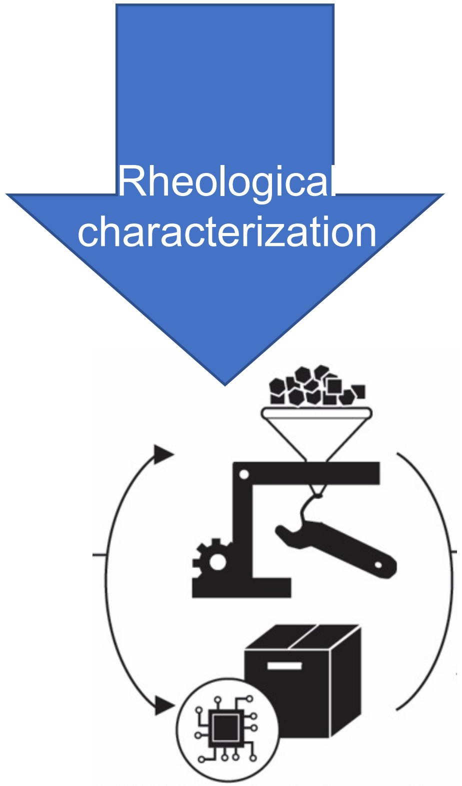

Santos, A. P., *et al.* (2020). Granular packings with sliding, rolling, and twisting friction. *Phys. Rev. E*, *102*(3), 32903.
Thompson, A. P., … Plimpton, S. J. (2022). LAMMPS … . *Comp. Phys. Comm.*, *271*, 108171.
Srivastava, I., *et al.* (2021). *Physical Review Research*, *3*(3), L032042.

Methods and model

Discrete element, particle-based modeling (DEM) (implemented within LAMMPS).

$P = 10^{-4}$

Monodisperese, frictional spheres

N=300 to 100,000 particles

Pressure P=10^{-2} to 10^{-6}

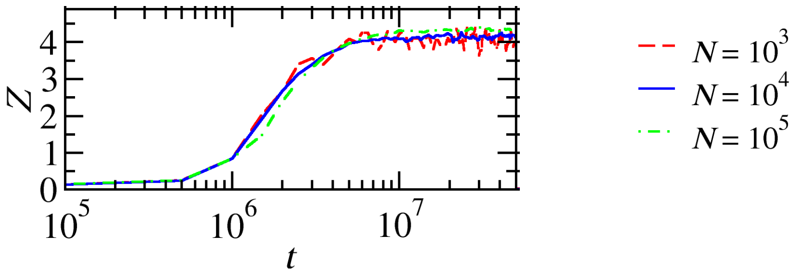

Plimpton S. (1995). *J. Comput. Phys.*, 117, 1-19.

Simulation protocol: specify stress tensor and bring dilute system to steady flowing state.

$$I = \dot{\gamma} d \sqrt{\rho / P}$$

$$\mu = \tau / P$$

$$\phi = V_p / V_t$$

$$Z = N_{\text{contacts}} / N_p$$

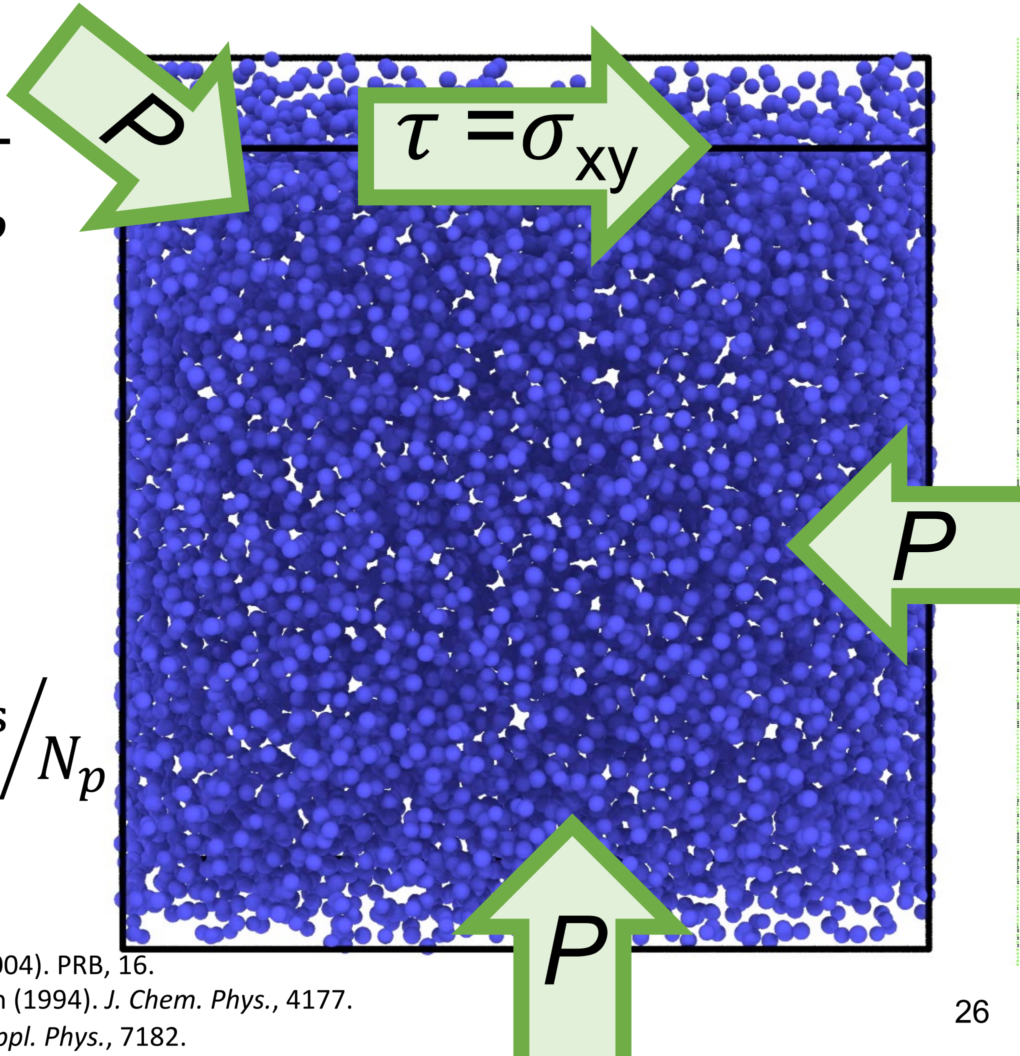

W. Shinoda, M. Shiga, and M. Mikami (2004). PRB, 16.
G. J. Martyna, D. J. Tobias, and M. L. Klein (1994). *J. Chem. Phys.*, 4177.
M. Parrinello and A. Rahman (1981). *J. Appl. Phys.*, 7182.

Dilation due to friction and flow

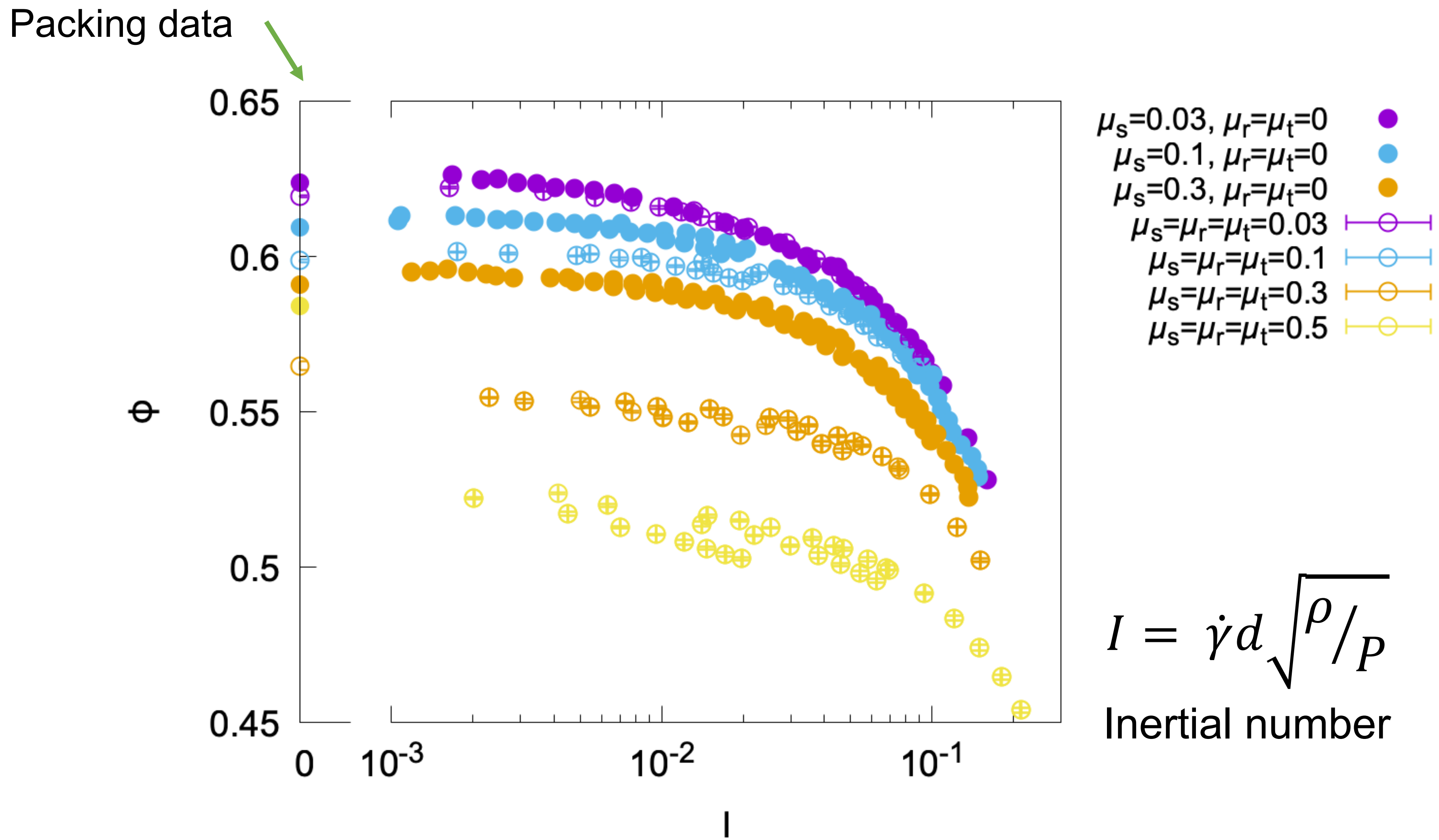

$$I = \dot{\gamma} d \sqrt{\rho / P}$$

Inertial number

- High sliding, rolling and twisting friction decrease the volume fraction

Srivastava, I., *et al.* (2019). *Phys. Rev. Lett.*, *122*(4), 48003.
Srivastava, I., *et al.* (2021). *J. Fluid Mech.*, 907, A18.

Santos *et. al. in preparation*

More shear stress is need to flow frictional particles

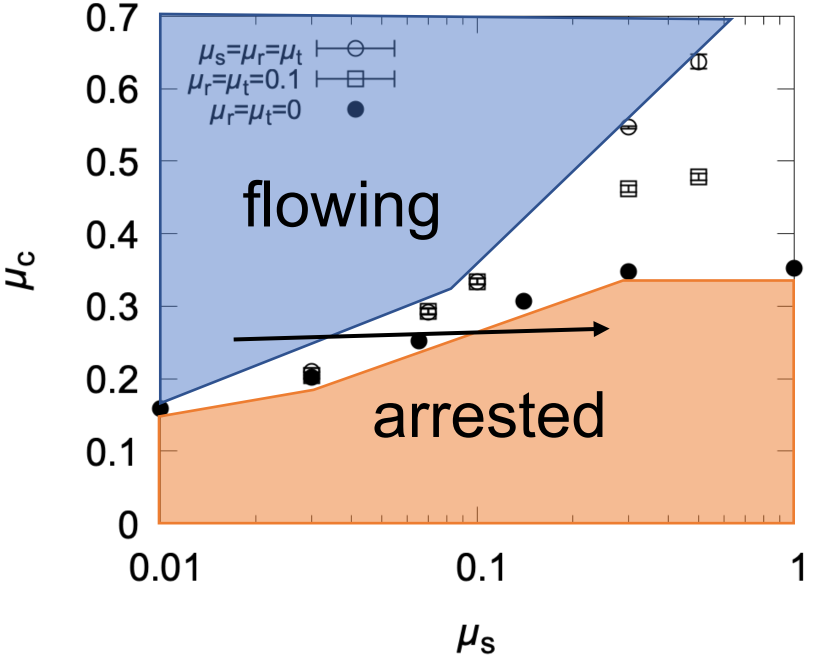

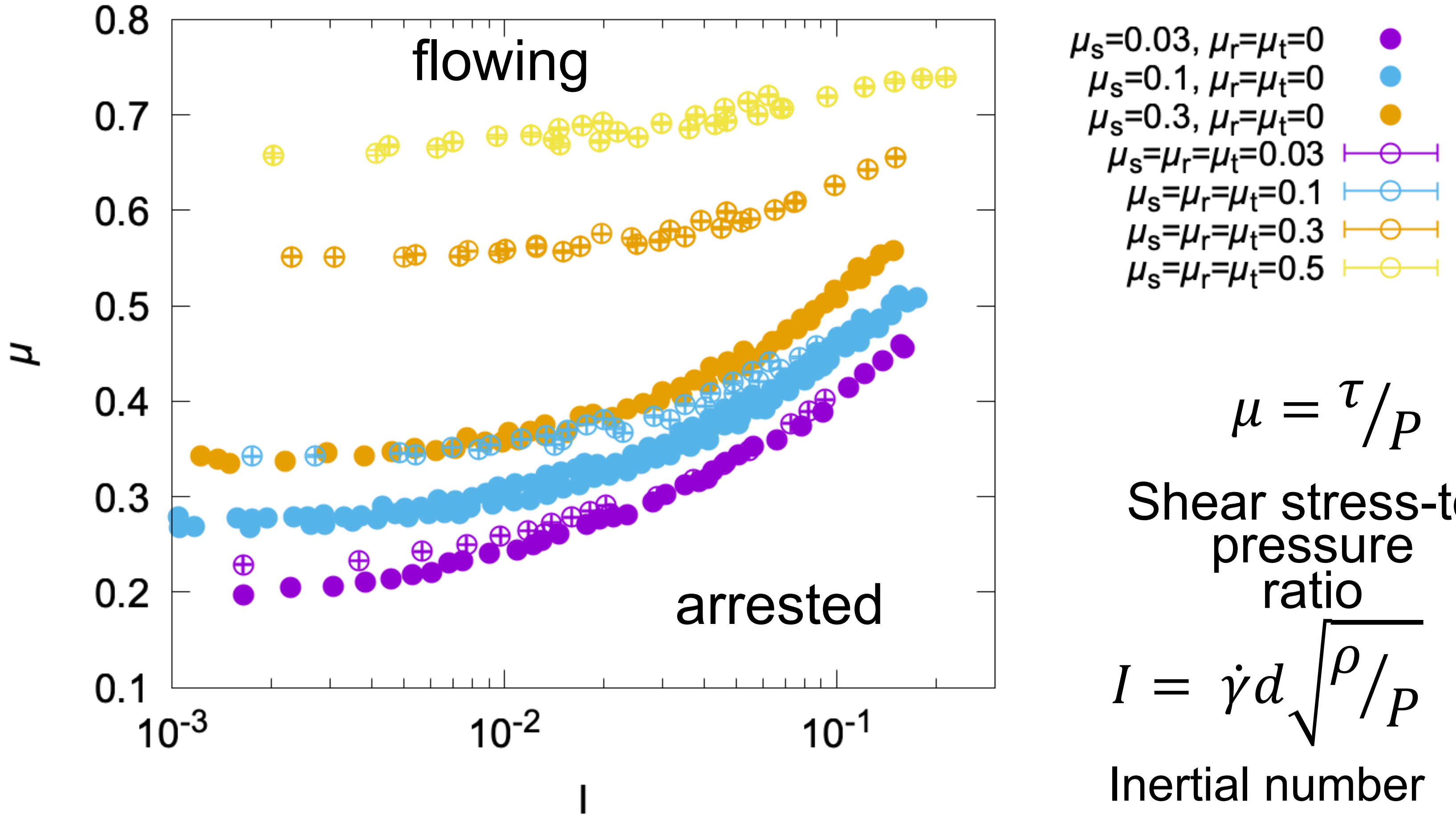

$$\mu = \tau/P$$

Shear stress-to-pressure ratio

$$I = \dot{\gamma} d \sqrt{\rho/P}$$

Inertial number

- High sliding, rolling and twisting friction increases the critical stress ratio
- A flowing frictionless system would arrest if the particles were frictional

Srivastava, I., *et al.* (2019). *Phys. Rev. Lett.*, *122*(4), 48003.
Srivastava, I., *et al.* (2021). *J. Fluid Mech.*, 907, A18.

Santos *et. al. in preparation*

Conclusions

- Rolling and twisting friction increase the critical flow shear stress ratio μ_c from 0.12 to 0.65
- A change in particle design can result in arrested flow

Acknowledgments

Ishan Srivastava, Dan S. Bolintineanu, Jeremy B. Lechman, Gary S. Grest, Steven J. Plimpton, Leonardo E. Silbert

Thermal Protection Materials Branch

Develop …
thermal protection materials …
to protect space vehicles from aerodynamic heating during entry to planet atmosphere and re-entry to earth atmosphere.

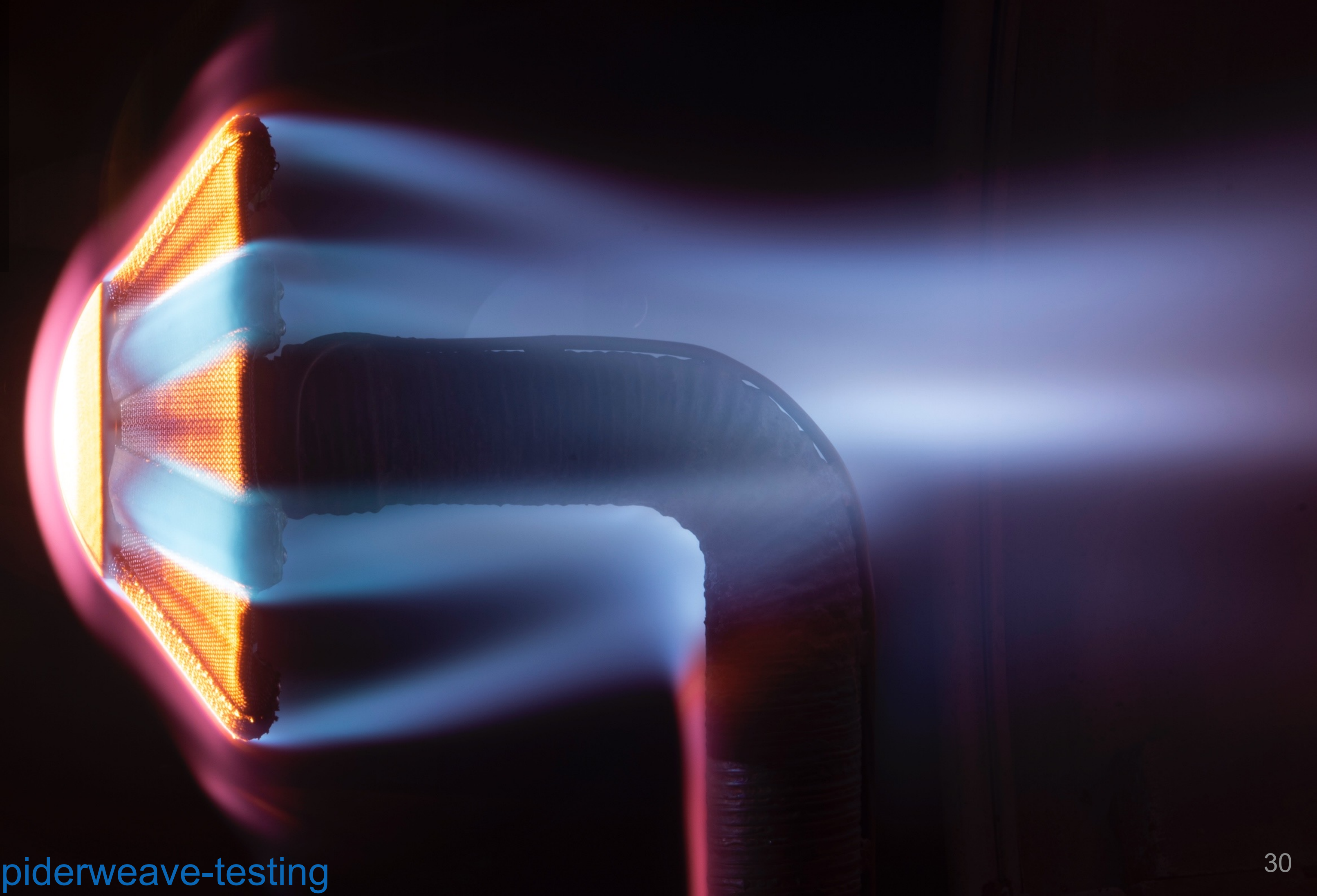

https://www.nasa.gov/image-feature/ames/spiderweave-testing

Current projects

Fiber modeling

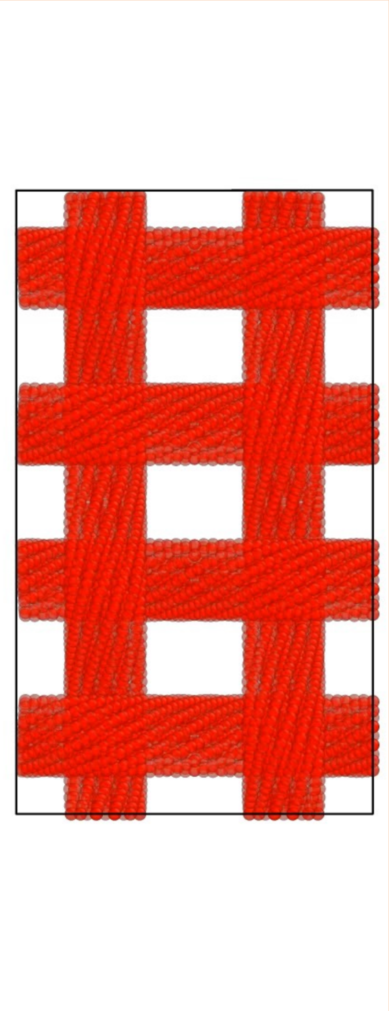

- Breakable bonds
- Friction
- Processing
- Mechanical and thermal properties

Molecular crystals

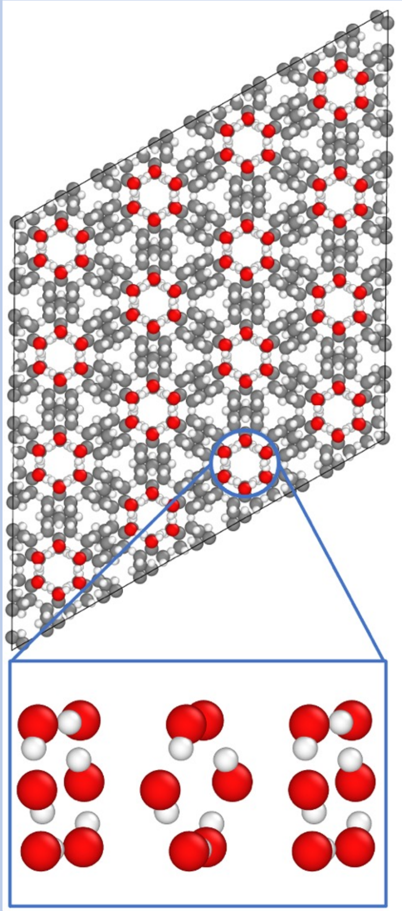

- Plastic crystals
- Barcaloric effects
- Cooling

Grafted microparticles

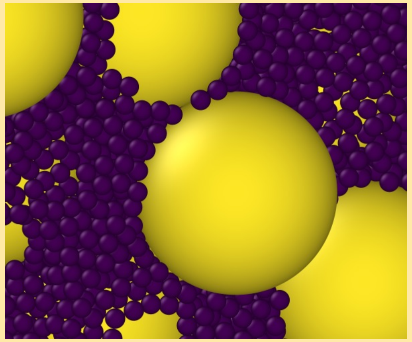

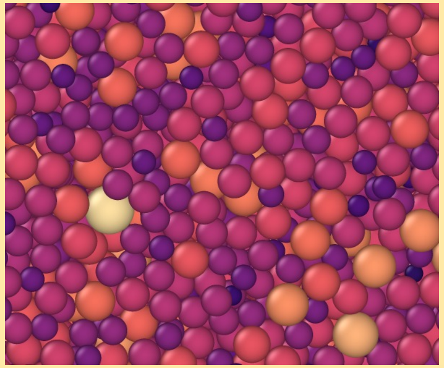

- Particle size
- Contacts
- Cohesion
- Friction
- Mechanical properties

Thank you!

- Increasing size dispersity (for f_a=0.27):
  - Increases the volume fraction
  - Decreases the A-B contact number
- Rolling and twisting friction:
  - Is required to match experimental volume fractions
  - change the packing microstructure
  - increase the critical flow shear stress ratio μ_c from 0.12 to 0.65

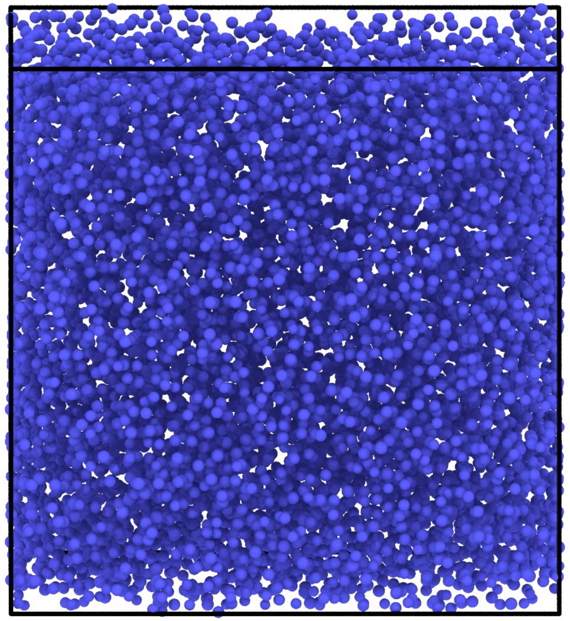

- Recommendations:
  - If $D_a = D_b$ use a 50:50 A:B mixture
  - If $D_a < D_b$ use a 73:27 A:B mixture
  - If the packing process is gentle: less friction is better (more contacts)
  - Low-friction particles improve flowability

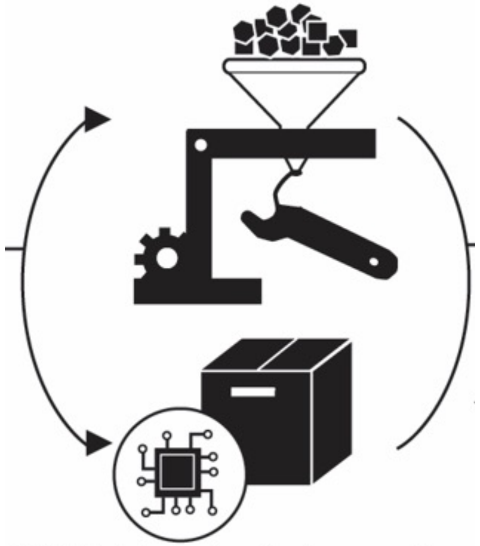

Extra slides

Packings and flow of granular particles

Natural processes

- Landslides and avalanches
- Shale
- Log jams
- Dunes

Manufacturing

- Battery anodes
- Concrete
- Candy
- Additive manufacturing

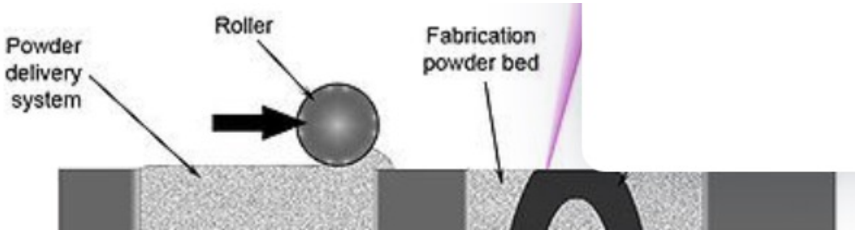

Past projects

Surfactants[1]

nonionic

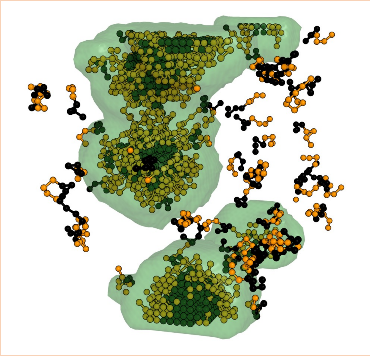

ionic

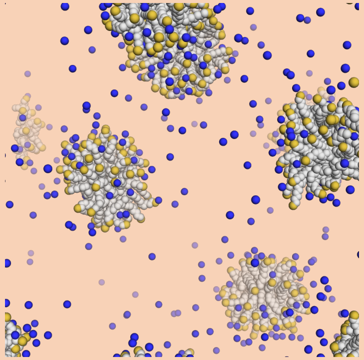

SALR Colloids

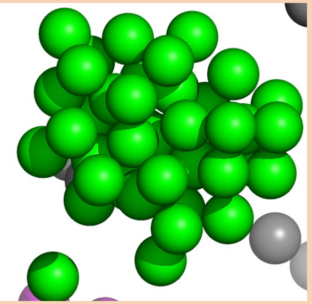

- Directly compare to experiments
- Quantified concentration effects
- Clarified self-assembly of SALR

Nanocomposites[2]

Grafted-NP

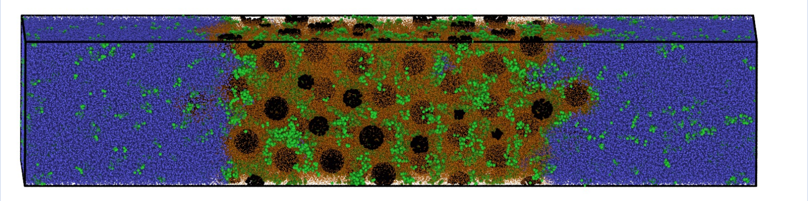

Magnetic

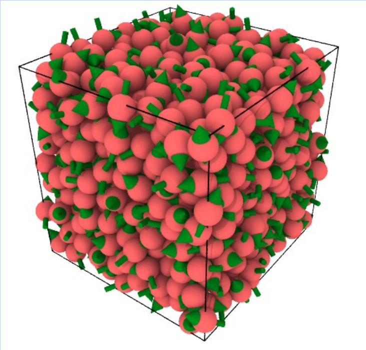

Bare NPs

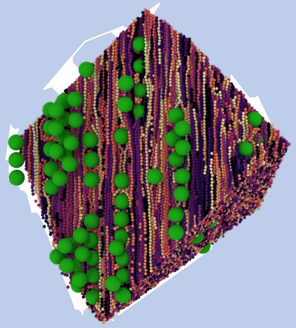

- Connect structure and phase behavior using large simulations
- Implemented new method

Granular[2]

Packings

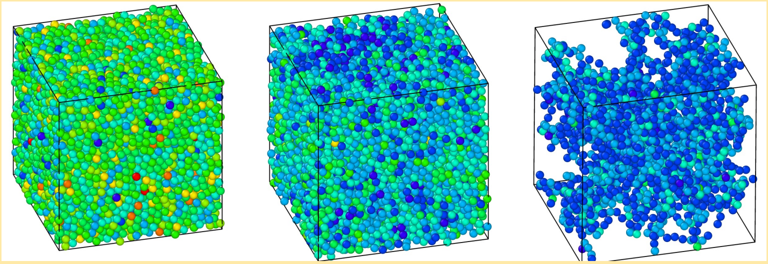

Flow

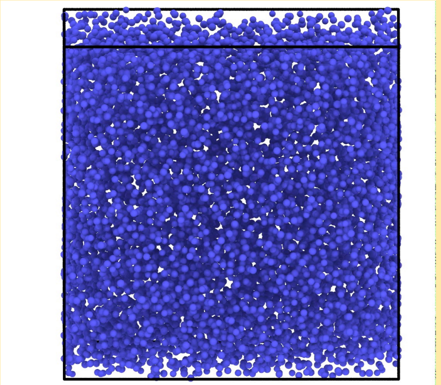

- Rolling/twisting friction
- Flow and packing

[1]PhD work at Princeton University in the Chemical and Biological Engineering Dept. [2]Postdoc work at Sandia National Labs.

Volume fraction

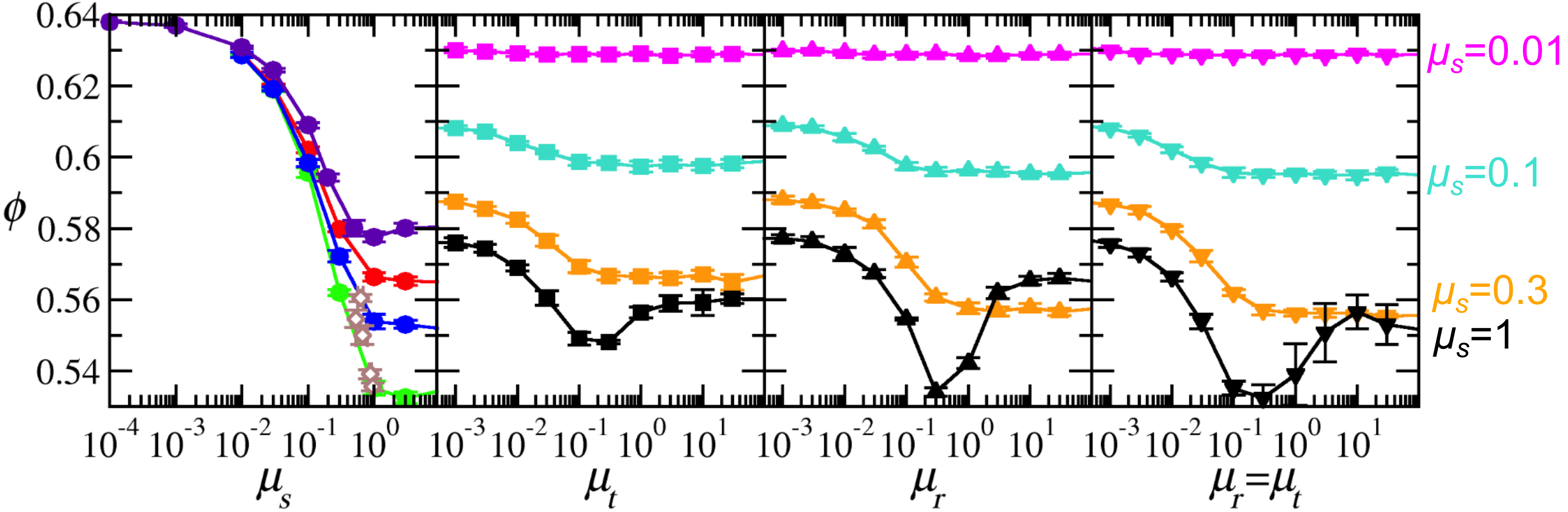

- Experiments are matched when moderate rolling and twisting friction are included
- Rolling and twisting friction have little effect for low μ_s
- ϕ minima at high $\mu_{s,r,t}$ may be due to large fraction of sliding contacts

Fraction of rattlers

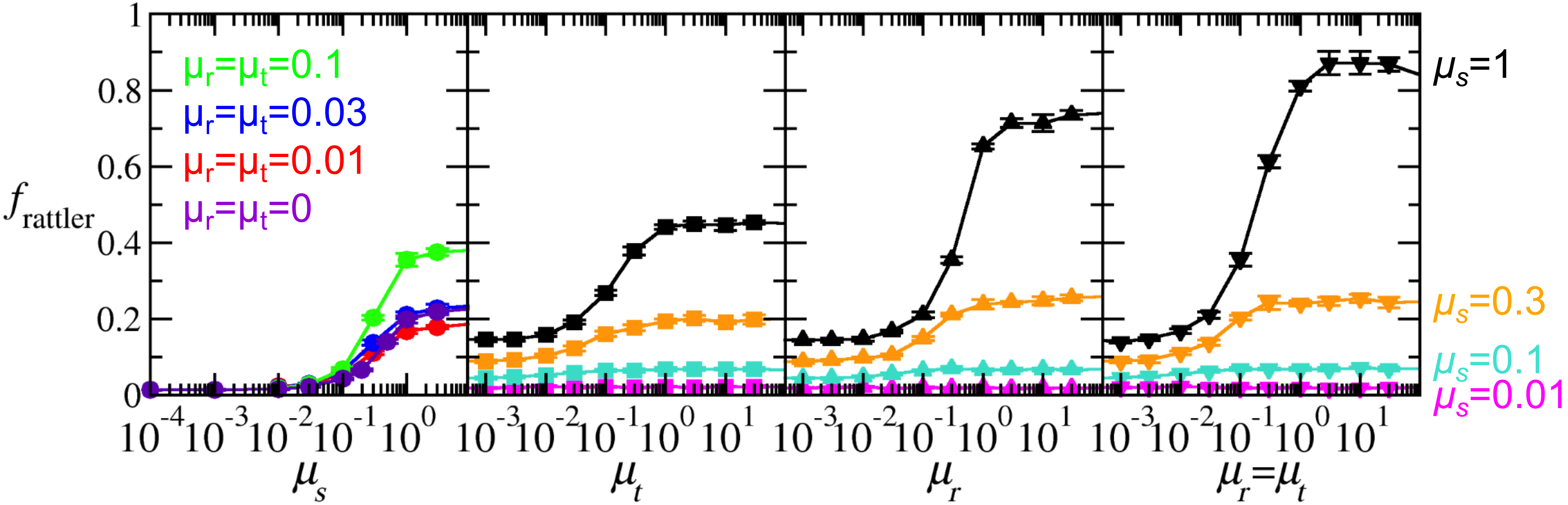

Volume fraction increases with dispersity

Furnas model:

$$\lim_{\alpha\to\infty}\phi_J(f^s)\begin{cases}\phi_J^{\text{mono}}/(1-f^s) & f^s<\left(1-\phi_J^{\text{mono}}\right)/\left(2-\phi_J^{\text{mono}}\right)\\ \phi_J^{\text{mono}}/\left[f^s+\phi_J^{\text{mono}}(1-f^s)\right] & f^s\geq\left(1-\phi_J^{\text{mono}}\right)/\left(2-\phi_J^{\text{mono}}\right)\end{cases}$$

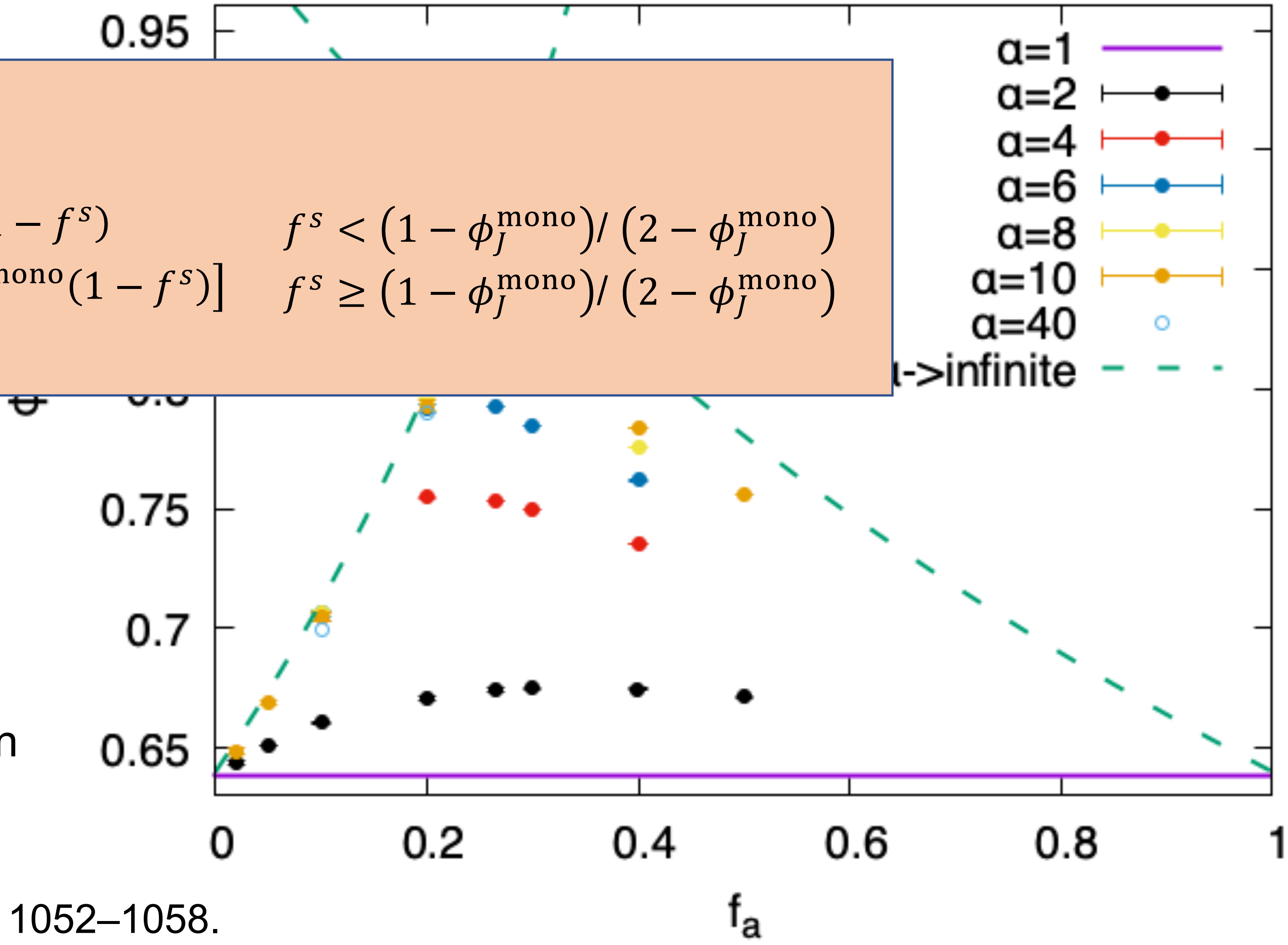

- Agreement with previous results
  - Shows hertzian and hookean have similar bidisperse packing behavior
- Larger size ratio -> lower void fraction -> more strength

Furnas, C. C. *Ind. Eng. Chem.* **1931**, *23* (9), 1052–1058.
Srivastava, I. *et al*. *Phys. Rev. Research* **2021**, *3* (3), L032042.

Multi-scale problems require multi-scale tools

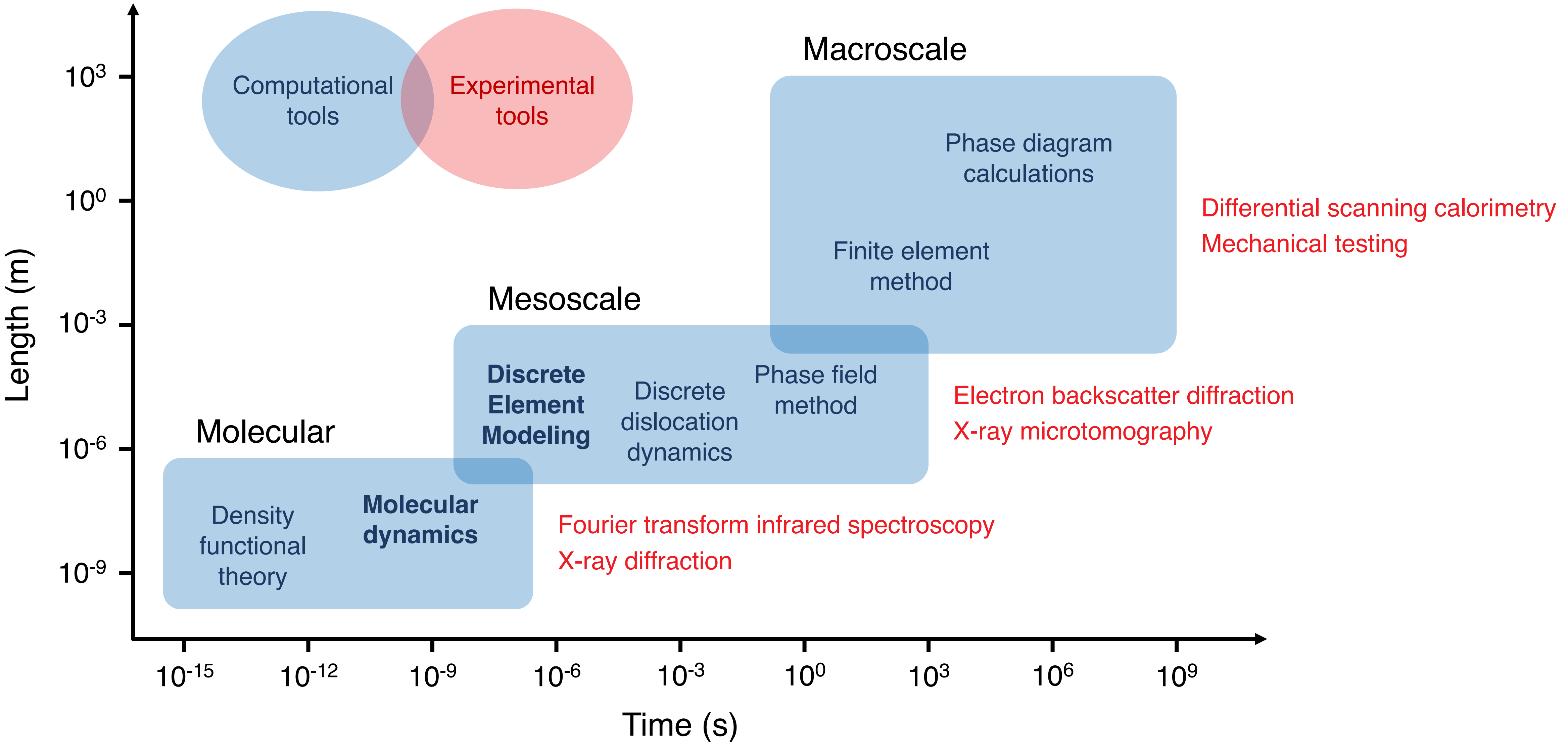

Coordination number

arXiv:2201.0368… (20…

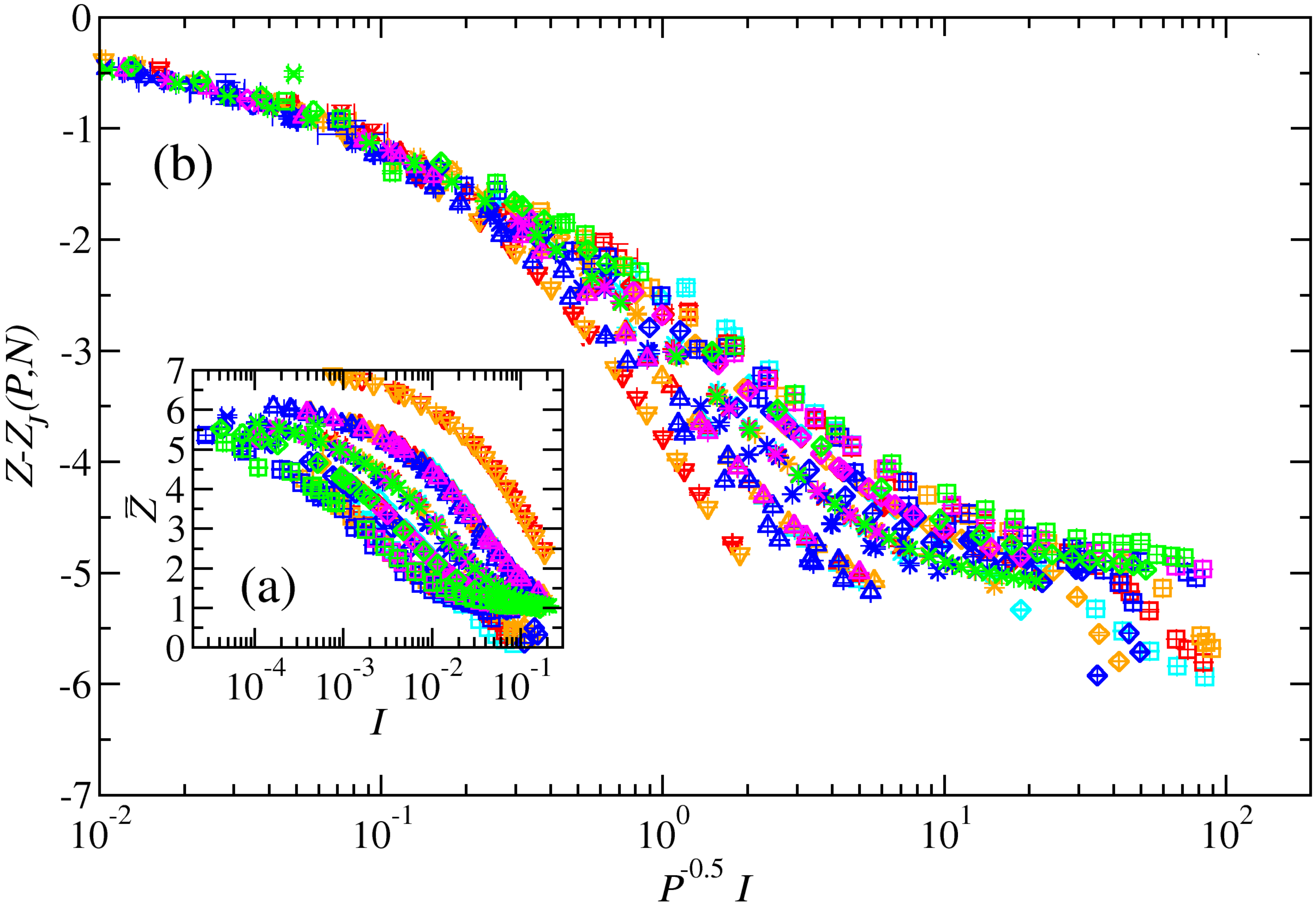

- *Average Z* is *P*-dependent, but *fluctuations* of *Z* is not
- *Z(I)* is *P*-dependent, but μ*(I)* and ϕ*(I)* are not
- Inertial number scales with $P^{-0.5}$ for ΔZ*(I)*
- Remove the hard-component for full collapse

$$Z = {N_{\text{contacts}}}\big/{N_p}$$

Shear stress ratio

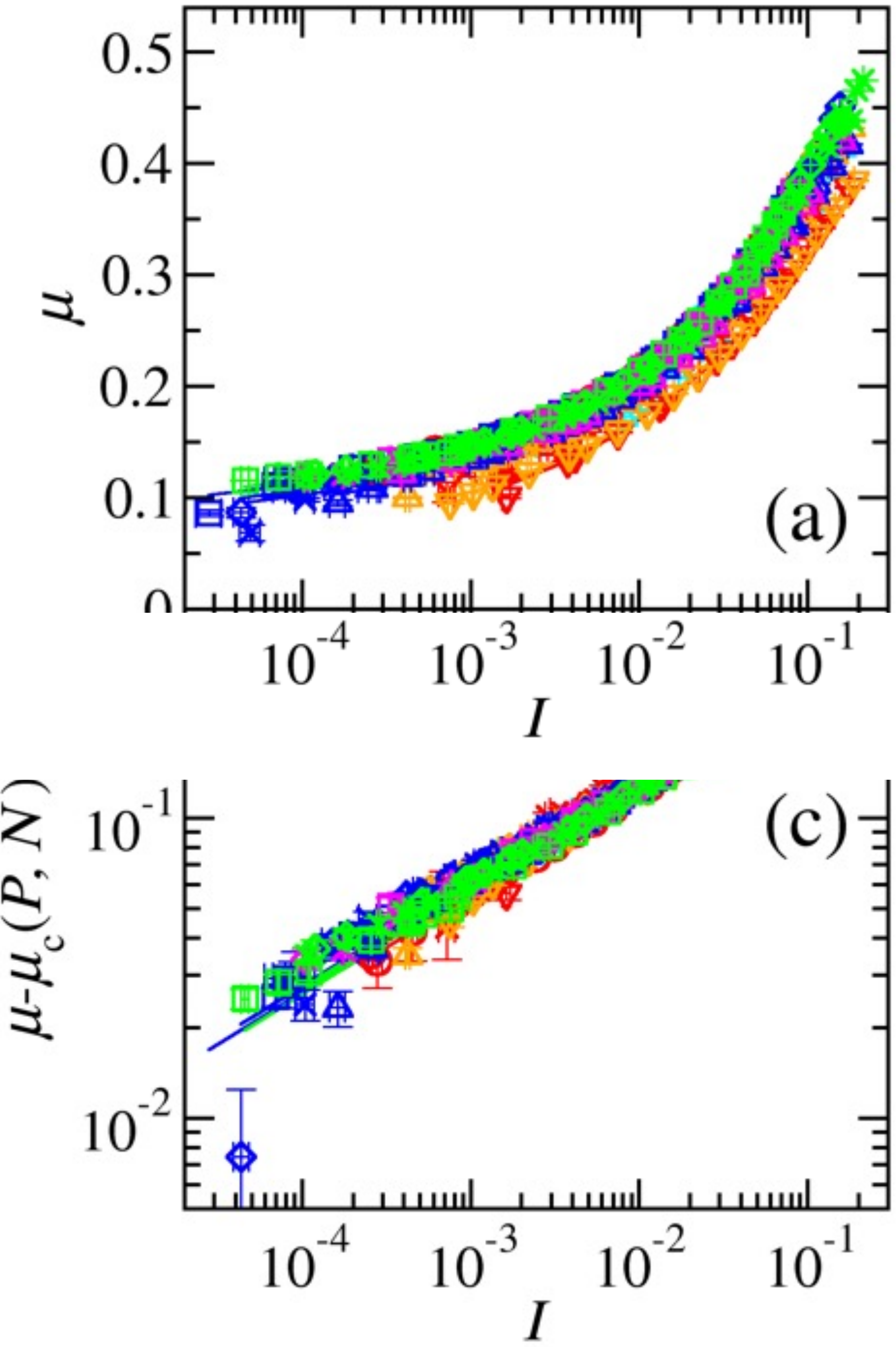

$$\mu = {}^{\tau}/_{P}$$

shear-to-pressure ratio

$$I = \dot{\gamma} d \sqrt{{}^{\rho}/_{P}}$$

Inertial number

- A power law fits the $\mu(I)$ data wel

Santos, A. P. *et al. in review* (2022)

Power-law fits

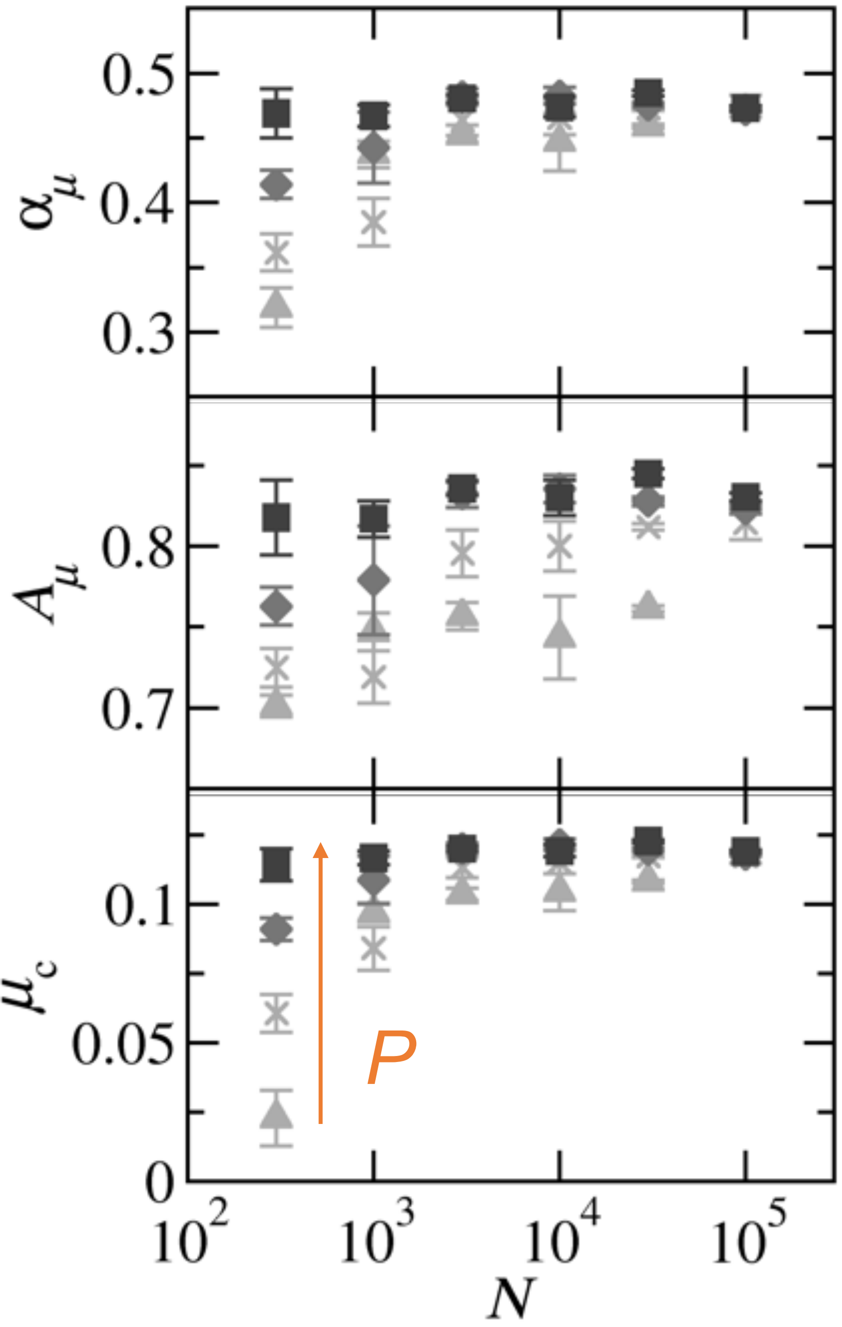

$$\mu = {}^{\tau}/_{P} = \mu_c + A_\mu I^{\alpha_\mu}$$

- Fit properties converge for large $N \geq 3000$
- The fit and arrest critical stress are distinct and size/pressure-dependent

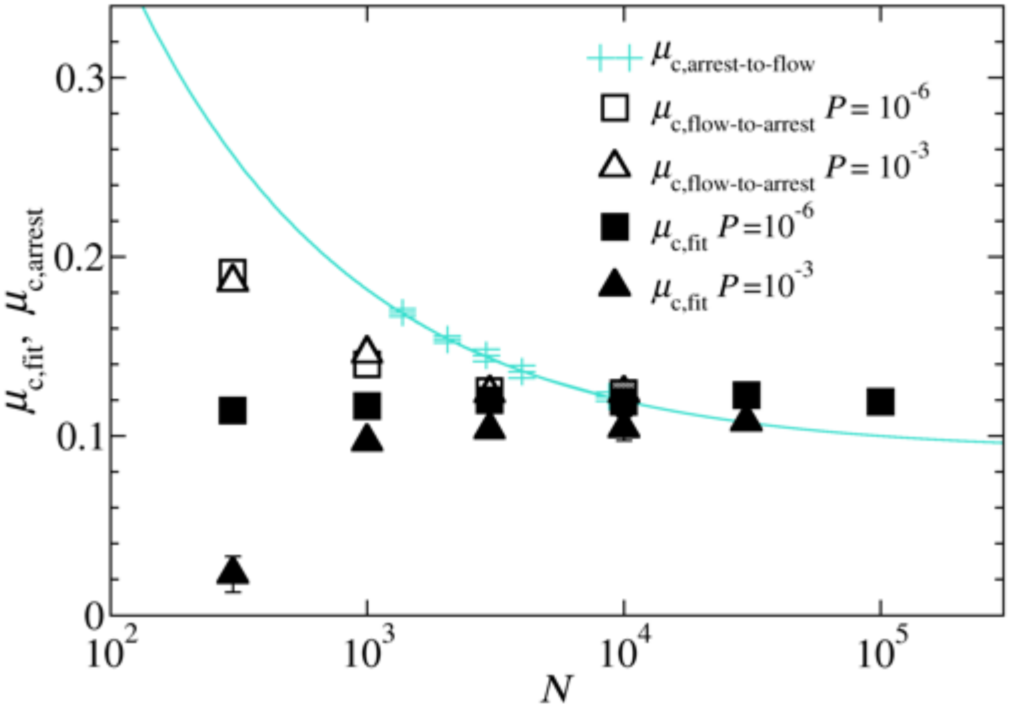

Pierre Emmanuel Peyneau *et al.* Phys. Rev. E 78, 011307 (2008).
Ishan Srivastava, *et al.* Phys. Rev. Lett. 122, 048003 (2019).
Santos, A. P. *et al. in review* (2022)

Normal stress differences

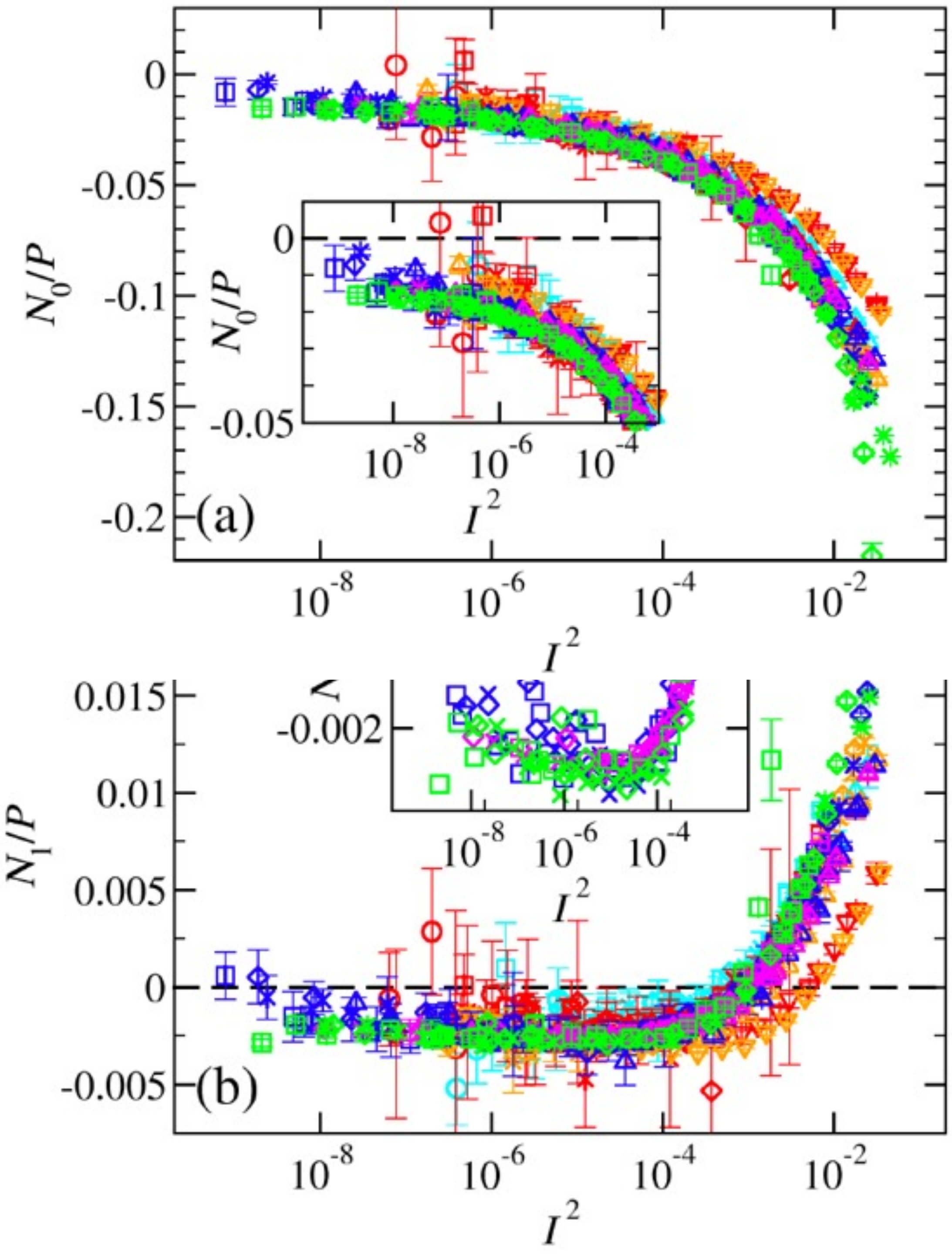

$$N_0 = \frac{2\sigma_{zz} - \sigma_{yy} - \sigma_{xx}}{2P}$$

$$N_1 = \frac{\sigma_{yy} - \sigma_{xx}}{P}$$

- N_0 is system size independent for $P \leq 10^{-4}$
- $N_0 \neq 0$ in the quasi-static limit
- N_1 has a minimum in I^2, only detectable for large systems $N \leq 10^4$

Srivastava, I. *et al.,* J. Fluid Mech. 907, A18 (2021).
Santos, A. P. *et al.* “Fluctuations and power-law scaling of dry, frictionless granular rheology near the hard-particle limit” *in review* (2022)

Fluctuations

Santos, A. P. *et al. in review* (2022)

$$\Delta\tau \equiv \frac{1}{N_{\text{samp}}}\Sigma_{i=1}^{N_{\text{samp}}}\left(\tau(t)-\bar{\tau}\right)$$

□ $N = 10^3$, $P = 10^{-6}$
◇ $N = 10^3$, $P = 10^{-5}$
× $N = 10^3$, $P = 10^{-4}$
□ $N = 10^4$, $P = 10^{-6}$
◇ $N = 10^4$, $P = 10^{-5}$
× $N = 10^4$, $P = 10^{-4}$
□ $N = 10^5$, $P = 10^{-6}$
◇ $N = 10^5$, $P = 10^{-5}$
× $N = 10^5$, $P = 10^{-4}$

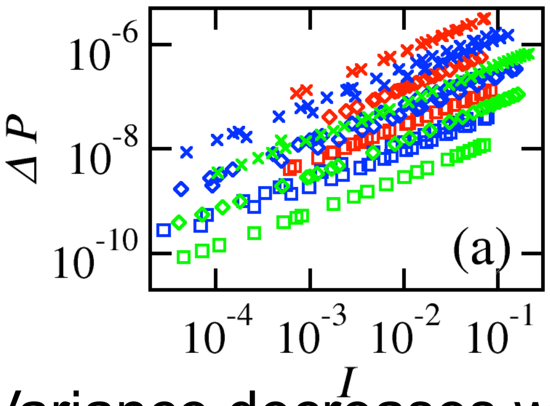

- Variance decreases with system size
  - There is a kink in fluctuations for shear stress, fabric anisotropy and normal stress differences
- Structure fluctuations show no *P* dependence

Fluctuations, normalized

Santos, A. P. *et al. in review* (2022)

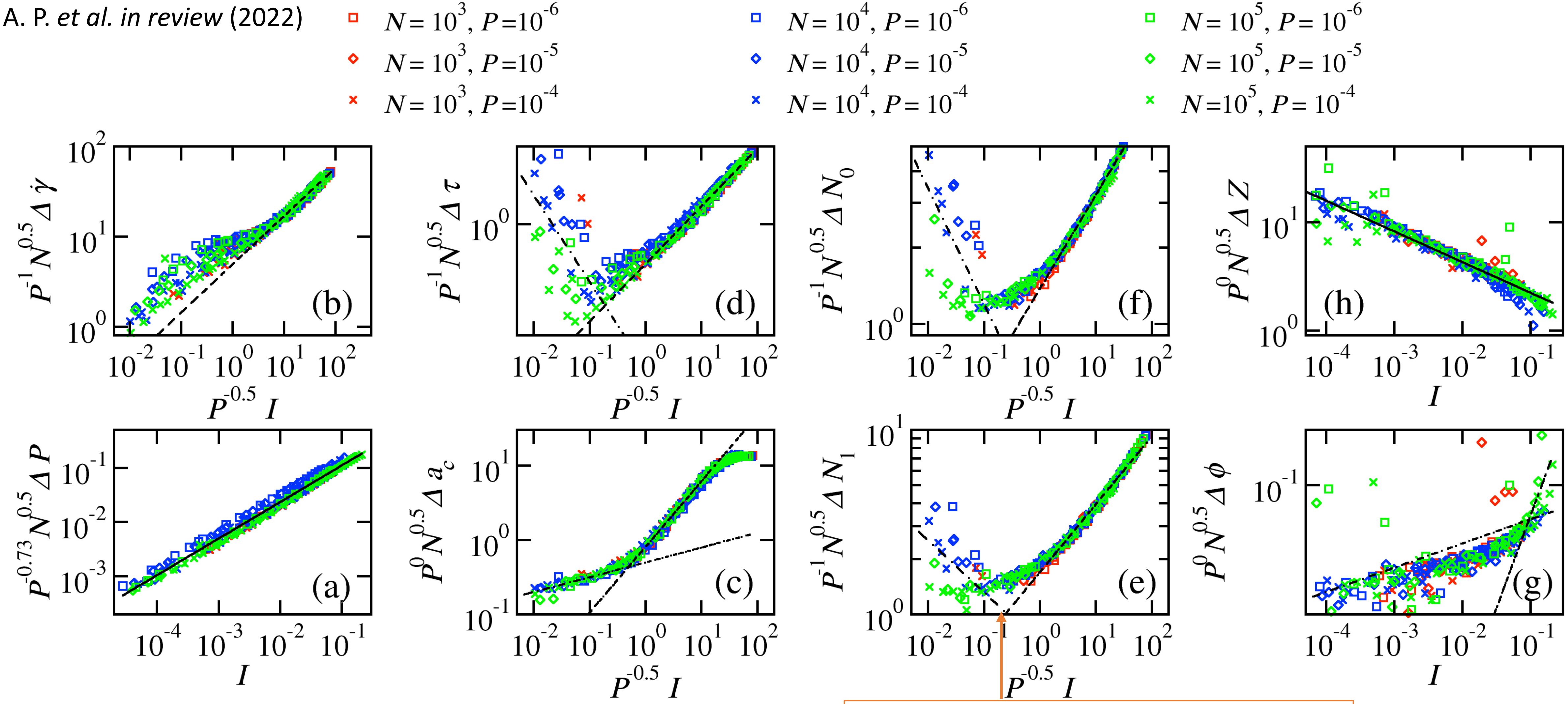

Could define the transition from inertial to quasi-static flow

- The kink is pressure dependent and scales as $P^{-0.5}$.
- Fluctuations scale with $N^{0.5}$ and $P^{-1}, P^{-0.73}$ or P^{0}

Conclusions

- Fluctuations across
- The observed kink in variance could define the transition from inertial to quasi-static flow

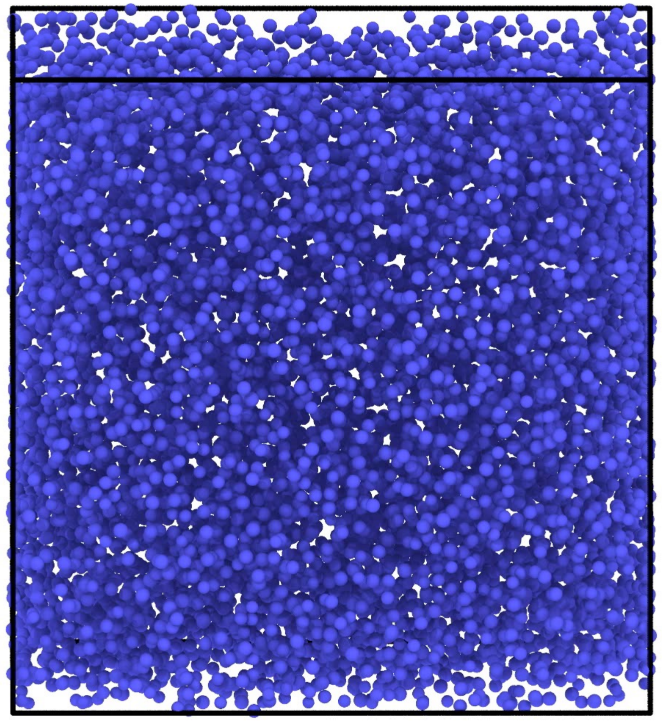

Future work

- **System size effects on the flow-arrest transition**
- **Further investigation into the connection between *Z* and variance**

More realistic interactions – cohesion and friction

- More constraints (friction, cohesion) -> lower volume fraction

$\alpha = \frac{D_{\text{large}}}{D_{\text{small}}} = 2 \qquad f_{\text{small}} = 0.02$

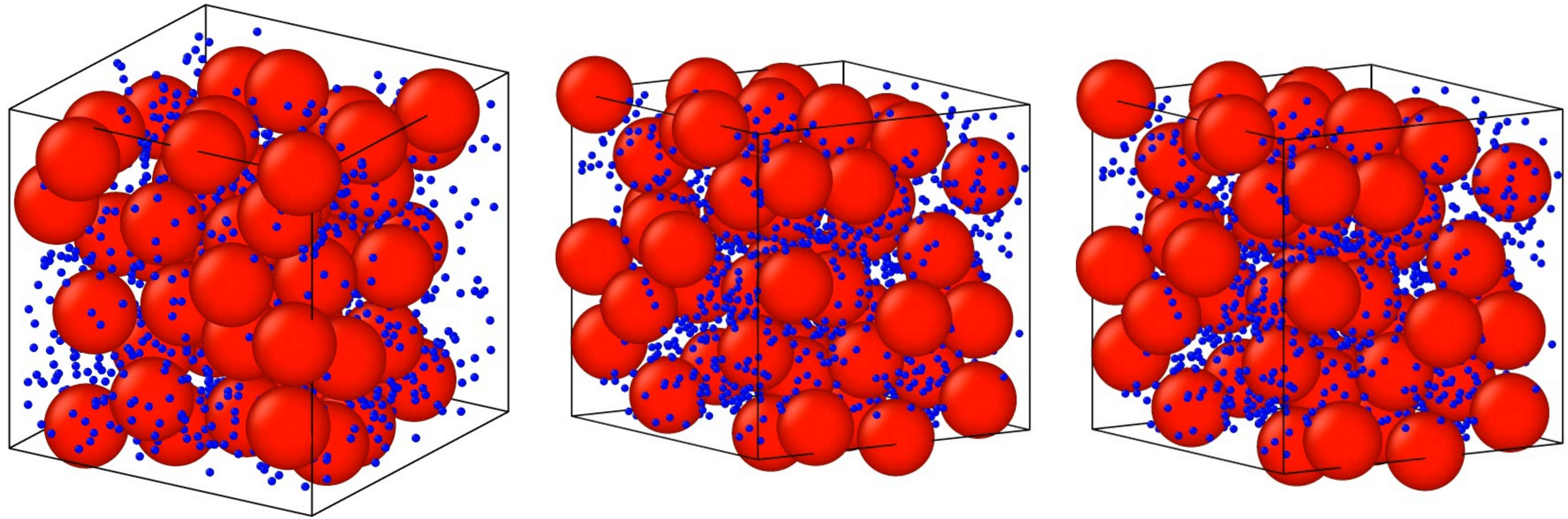

Frictionless, cohesionless | Frictionless, cohesive | Frictional + cohesive

Current projects

Fiber modeling

Bonded-particle models
- Forces calculated at contact
- Requires memory of interaction
- Dissipative, out-of-equilibrium
- LAMMPS

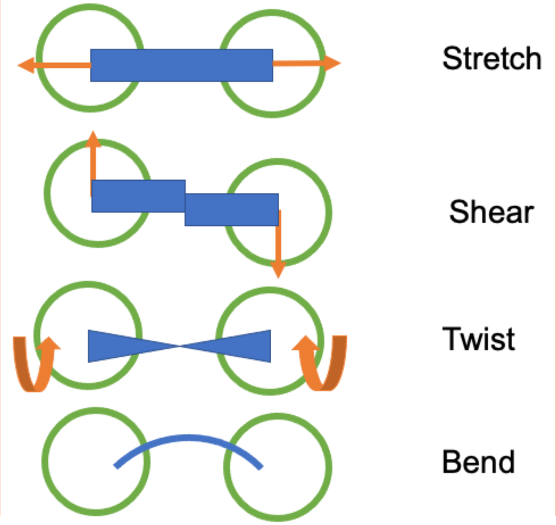

Molecular crystals

Molecular Dynamics (MD)
- *NPT* ensemble
- Gromacs

Model
- Atomistic
- Classical potentials

Grafted microparticles

Discrete element modeling (DEM)
- Forces calculated at contact
- Requires memory of interaction
- Dissipative, out-of-equilibrium
- LAMMPS

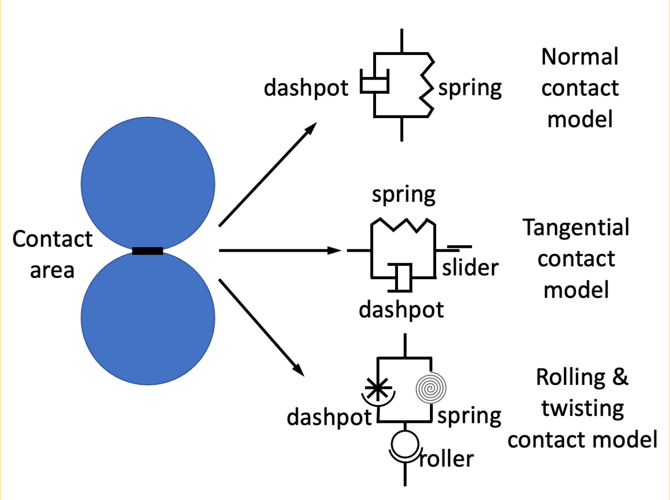

Past projects

Surfactants

Molecular Dynamics (MD)

- *NVT* ensemble
- Gromacs, Hoomd, LAMMPS

Monte Carlo (MC)

- Cassandra, Legacy code (Fortran)
- Develop MC moves and potentials
- *μVT, NVT* ensembles
- Histogram reweighting

Law-of-mass-action modelling

Nanocomposites

Molecular dynamics
Theoretically-informed Langevin dynamics (TILD)

- MD evolves simulation of particles
- Force on particle is calculated from a field-based interaction
- Fast for dense systems
- Thermal fluctuations
- Implemented into LAMMPS

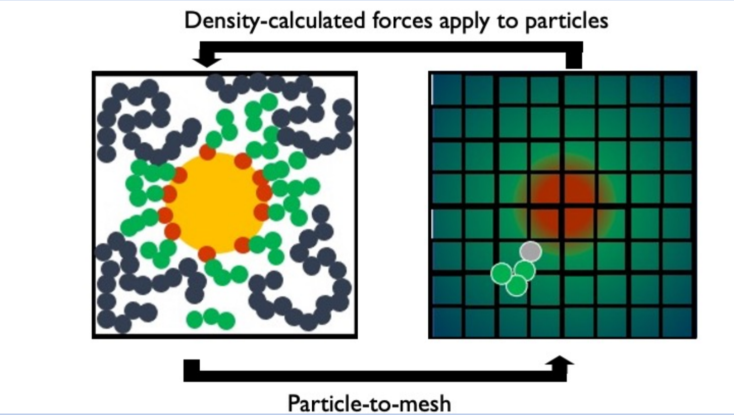

Granular

Discrete element modeling (DEM)

- Forces calculated at contact
- Requires memory of interaction
- Dissipative, out-of-equilibrium
- LAMMPS